



Article

# The Monocytic Cell Line THP-1 as a Validated and Robust Surrogate Model for Human Dendritic Cells

Johanna Maria Hölken and Nicole Teusch \*

Institute of Pharmaceutical Biology and Biotechnology, Heinrich-Heine University Düsseldorf,  
Universitätsstraße 1, 40225 Düsseldorf, Germany

\* Correspondence: nicole.teusch@hhu.de; Tel.: +49-211-81-14163

**Abstract:** We have implemented an improved, cost-effective, and highly reproducible protocol for a simple and rapid differentiation of the human leukemia monocytic cell line THP-1 into surrogates for immature dendritic cells (iDCs) or mature dendritic cells (mDCs). The successful differentiation of THP-1 cells into iDCs was determined by high numbers of cells expressing the DC activation markers CD54 (88%) and CD86 (61%), and the absence of the maturation marker CD83. The THP-1-derived mDCs are characterized by high numbers of cells expressing CD54 (99%), CD86 (73%), and the phagocytosis marker CD11b (49%) and, in contrast to THP-1-derived iDCs, CD83 (35%) and the migration marker CXCR4 (70%). Treatment of iDCs with sensitizers, such as NiSO<sub>4</sub> and DNCB, led to high expression of CD54 (97%/98%; GMFI, 3.0/3.2-fold induction) and CD86 (64%/96%; GMFI, 4.3/3.2-fold induction) compared to undifferentiated sensitizer-treated THP-1 (CD54, 98%/98%; CD86, 55%/96%). Thus, our iDCs are highly suitable for toxicological studies identifying potential sensitizing or inflammatory compounds. Furthermore, the expression of CD11b, CD83, and CXCR4 on our iDC and mDC surrogates could allow studies investigating the molecular mechanisms of dendritic cell maturation, phagocytosis, migration, and their use as therapeutic targets in various disorders, such as sensitization, inflammation, and cancer.

**Keywords:** dendritic cells; THP-1; DC maturation; cytokine; sensitization; phagocytosis; nickel sulfate; NiSO<sub>4</sub>; h-CLAT; 1-chloro-2,4-dinitrobenzene; DNCB; interleukin-12; IL-12



**Citation:** Hölken, J.M.; Teusch, N. The Monocytic Cell Line THP-1 as a Validated and Robust Surrogate Model for Human Dendritic Cells. *Int. J. Mol. Sci.* **2023**, *24*, 1452. <https://doi.org/10.3390/ijms24021452>

Academic Editor: Christopher W Cutler

Received: 17 November 2022

Revised: 5 January 2023

Accepted: 7 January 2023

Published: 11 January 2023



**Copyright:** © 2023 by the authors. Licensee MDPI, Basel, Switzerland. This article is an open access article distributed under the terms and conditions of the Creative Commons Attribution (CC BY) license (<https://creativecommons.org/licenses/by/4.0/>).

## 1. Introduction

Dendritic cells (DC) are sentinel leukocytes mediating the innate and adaptive immune response in mammalian solid tissue. Dendritic cells play fundamental roles in infections [1,2], inflammation [3], skin sensitization [4], and allergy [5], as well as in cancer [6–8] and are, therefore, of great interest in research [9]. The DCs are a heterogeneous population of cells, specialized in antigen presenting. Upon exposure to, for example, pro-inflammatory cytokines, such as tumor-necrosis factor alpha (TNF- $\alpha$ ), bacterial agents, such as lipopolysaccharides (LPS), or chemically-derived haptens, such as from nickel sulfate (NiSO<sub>4</sub>), maturation and migration of DCs is initiated. The DCs initially transform into immature dendritic cells (iDCs) with high endocytic activity and low T-cell activation potential [10,11]. The first steps of phagocytosis and maturation are accompanied by up-regulation of the major histocompatibility complex (MHC) class II, such as the Human Leukocyte Antigen–DR isotype (HLA-DR) [12,13]. The MHC II molecules are synthesized on the cytosolic surface of the endoplasmic reticulum and are chaperoned by the invariant chain (Ii) to the late endosomal compartment where they encounter and fuse with endosomes loaded with the exogenous protein of presenting, building lysosome-like antigen processing compartments [14–16]. In order to bind antigens, the Ii peptide is cleaved. After loading a peptide derived from the exogenous protein, the class II molecules are exported to the cell surface for recognition by CD4<sup>+</sup> T cells [15]. In addition, internalized antigens can be loaded onto MHC I molecules for cross-presentation to CD8<sup>+</sup> T cells [17,18]. Simultaneously, expression of adhesion molecules, such as clusters of differentiation (CD)54 and

co-stimulatory molecules, such as CD80 and CD86, are upregulated and transported to the cell surface, inducing dendritic cell maturation [19,20]. Furthermore, DC maturation is accompanied by upregulation of migration markers, such as the C-X-C chemokine receptor type 4 (CXCR4) and C-C chemokine receptor type 7 (CCR7), resulting in antigen presentation to T cells in lymphoid tissues [21,22]. Overall, migration of DCs is a complex process which depends on chemokines, such as stromal cell-derived factor 1 (SDF-1), chemokine (C-C motif) ligand (CCL) 19, and CCL21 [23–26]. The SDF-1 is secreted by fibroblasts and endothelial cells in the dermis after antigen exposure, inducing chemotactic migration of CXCR4-expressing DCs to lymphatic vessels in the dermis [23,24]. Contrarily, CCL19 and CCL21 are secreted by lymph nodes, inducing CCR7 dependent migration of DCs and naïve T cells [25–27].

The activation of naïve CD4<sup>+</sup> T cells is initiated by the interaction of T cell receptors (TCRs) with the antigen-loaded MHC II complexes [28,29]. However, to fully prime naïve CD4<sup>+</sup> T cells, the simultaneous interaction with DC-expressing CD54, CD80, and CD86 is required [30,31]. In order to form a stable signaling structure between dendritic cells and naïve CD4<sup>+</sup> T cells, the intracellular adhesion molecule (ICAM-1)/CD54 forms with its partners, leukocyte function-associated antigen 1 (LFA-1) alpha (CD11a) and beta-2 (CD18), a cell–cell adhesion, the so-called immunological synapse (IS) [32,33]. Subsequently, high expression of the surface molecules CD80 (B7-1) and CD86 (B7-2) on antigen-presenting cells (APCs) allows the co-stimulation of naïve CD4<sup>+</sup> T cells via their CD28 and cytotoxic T-lymphocyte-associated protein 4 (CTLA-4)/(CD152) receptors [34,35]. Upon the cell–cell contact between dendritic cells and T cells, several signal cascades in both T cells and dendritic cells are initiated, depending on the stability and duration of the cell–cell contact, and the number of MHC complexes and co-stimulatory molecules enhancing the transfer [36]. In immature dendritic cells, CD83 is not expressed on the cell surface, but is stored in the Golgi complex and endocytic vesicles, and the receptor can be transported to the cell surface immediately upon maturation [37,38]. Notably, CD83 knockout studies revealed a severe reduction in CD4<sup>+</sup> T cells, proving the essential role of CD83 for the development of CD4<sup>+</sup> T cells [39,40]. By binding to the membrane-associated RING-CH8 (MARCH-8) ubiquitin ligase, which is responsible for the internalization of MHC II, CD83 stabilizes the MHC II surface expression [41]. In addition, transmembrane regulation of the MARCH-1 ubiquitin ligase promotes the upregulation of surface MHC-II and CD86 on activated DCs [42,43], ensuring the stimulation, proliferation, and maturation of naïve T cells into primed effector and memory T-lymphocytes in the draining lymph nodes [44].

In the past decades, the predictive identification of potentially sensitizing agents has been performed via the guinea pig Buehler test or the murine lymph node assay LLNA. However, due to the differences between human and guinea pig/murine skin physiology and immune biology many agents were classified as false positive or negative [45,46]. Hence, there was an urgent need for alternative robust human-derived models. In this context, various protocols generating dendritic cell surrogates derived from human donor-derived peripheral blood monocytes (PBMCs) to study skin sensitization and inflammation have been reported [47–50]. However, the isolation and differentiation of PBMCs comes with various technical and biological limitations, such as the amount, availability, and donor heterogeneity [51,52]. In 2006, the human cell line activation test (h-CLAT) was developed by Ashikaga et al. [53,54]. The h-CLAT addresses one of the key events of the skin sensitization, by measuring CD54 and CD86 as markers for dendritic cell activation on the monocytic cell line THP-1 [53], originally isolated from peripheral blood of an acute leukemia patient [55]. The method is designed to distinguish between sensitizing and non-sensitizing agents, where the chemicals 1-chloro-2,4-dinitrobenzene (DNCB) and nickel sulfate (NiSO<sub>4</sub>), both acting as strong sensitizers, are the positive controls. In order to be classified as a sensitizer, the relative fluorescence intensity (RFI) has to exceed a defined threshold, which is CD54  $\geq$  200 or CD86  $\geq$  150 in at least two out of three independent measurements [56,57]. Due to high intra- and inter-laboratory reproducibility (80%) [57,58], the h-CLAT was validated and authorized by the European Union Reference

Laboratory on Alternatives to Animal Testing (EURL ECVAM) and by the Organization for Economic Co-Operation and Development (OECD) for the toxicological assessment of skin sensitization potential [58,59]. In conclusion, THP-1 cells bring along various advantages for differentiation into dendritic cell surrogates.

In most studies to date, THP-1 cells have been differentiated into macrophages [60,61], and only very few publications have converted THP-1 cells into iDCs and mDCs (Table 1). Similar to human PBMCs, THP-1 cells could be differentiated into iDCs with cytokines, such as GM-CSF and IL-4 [62–65]. Maturation of THP-1 into mDCs was achieved via GM-CSF, IL-4, TNF- $\alpha$ , and ionomycin exposure in (serum-free) medium for 24 h to 72 h [62,66], or by cultivating THP-1-derived iDCs for an additional 24–72 h in (serum-free) medium supplemented with GM-CSF and/or IL-4, TNF- $\alpha$ , and ionomycin [64,65]. However, as these protocols differ in cell numbers, basic media composition, media supplementation, the number of days for differentiation, the frequency of media exchange and, most importantly, the cytokine concentrations in the differentiation cocktail, it becomes highly challenging to identify the appropriate method.

**Table 1.** Literature review of the differentiation of THP-1 into iDCs or mDCs.

Cultivation Conditions	iDCs	mDCs	Ref.
Cytokine concentrations	100 ng/mL (1500 U/mL) GM-CSF 100 ng/mL (1500 U/mL) IL-4	100 ng/mL (1500 U/mL) GM-CSF 200 ng/mL (3000 U/mL) IL-4 20 ng/mL (2000 U/mL) TNF- $\alpha$ 200 ng/mL ionomycin	[62]
Medium	RPMI, 10% serum,	RPMI, serum-free,	
Cell number	$2 \times 10^5$ cells/ ml, 20 mL	$2 \times 10^5$ cells/ ml, 20 mL	
Time of differentiation	5 d of cultivation	24–72 h of cultivation Exposure of generated iDCs to	
Cytokine concentrations	150 ng/mL GM-CSF 50 ng/mL IL-4	10 ng/mL IL-1 $\beta$ 10 ng/mL TNF- $\alpha$ 2 $\mu$ g/mL PGE <sub>2</sub> 25% MCM Or 1 $\mu$ g/mL LPS	[63]
Medium	RPMI, 10% serum,	RPMI, 10% serum	
Cell number	$5 \times 10^5$ cells/ ml	Cell number not indicated	
Time of differentiation	7 d of cultivation	48 h of cultivation	
Cytokine concentrations	-	100 ng/mL (1500 U/mL) GM-CSF 200 ng/mL (3000 U/mL) IL-4 20 ng/mL (3000 U/mL) TNF- $\alpha$ 200 ng/mL ionomycin	[66]
Medium	-	DMEM, serum-free	
Cell number	-	$2 \times 10^5$ cells/ ml, 20 mL	
Time of differentiation	-	48 h of cultivation Exposure of generated iDCs to:100 ng/mL	
Cytokine concentrations	100 ng/mL GM-CSF 100 ng/mL IL-4	GM-CSF 100 ng/mL IL-4 20 ng/mL TNF- $\alpha$ 200 ng/mL ionomycin	[64]
Medium	RPMI, 10% serum	RPMI, serum-free	
Cell number	Not indicated	Not indicated	
Time of differentiation	5 d of cultivation	72 h of cultivation Exposure of generated iDCs to:	
Cytokine concentrations	1500 U/mL GM-CSF 1500 U/mL IL-4	3000 U/mL IL-4 2000 U/mL TNF- $\alpha$ 200 ng/mL ionomycin	[65]
Medium	RPMI, 10% serum	RPMI, 10% serum	
Cell number	$2 \times 10^5$ cells/mL, 20 mL	Not indicated	
Time of differentiation	5 d of cultivation	24 h of cultivation	

Thus, our aim was to establish robust and highly reproducible standard operating procedures addressing THP-1-derived iDC and mDC surrogates for in vitro toxicological studies as well as for investigating the underlying mechanisms of human skin sensitization and inflammation.

## 2. Results

The differentiation of THP-1 cells into dendritic cells has been described using RPMI or DMEM as a cultivation medium (Table 1). Both RPMI and DMEM are basal mediums which do not contain proteins or growth promoting agents and, as such, require supplementation with a serum, such as FBS. However, RPMI contains high concentrations of vitamins, as well as amino acids, such as asparagine, proline, biotin, and vitamin B12, which are not incorporated in DMEM [67]. On the other hand, DMEM contains higher concentrations of calcium (1.8 mM) and a lower concentration of phosphate (1 mM), compared to RPMI (0.8 mM calcium, 5 mM phosphate, respectively). While DMEM is selected for adherent cells, RPMI is widely used for suspension cells [68–70]. In line with this, RPMI is the recommended culture medium by the American Type Culture Collection (ATCC) and Deutsche Sammlung von Mikroorganismen und Zellkulturen (DSMZ) for THP-1 cells. Furthermore, PBMCs cultured in RPMI showed more efficient differentiation into DCs compared to PBMCs cultured in DMEM [71]. Based on these specifications, we decided to implement our differentiation protocols using RPMI.

The differentiation of THP-1 into iDCs and mDCs has been described using cytokine concentrations in ng/mL or in U/mL concentrations. However, by converting the indicated cytokine concentrations from ng/mL into U/mL and vice versa for the cytokines to be supplemented (Table 2), apparently significant differences become obvious. Thus, to systematically compare supplementation differences, we differentiated THP-1 cells into iDCs and mDCs by supplementing the medium with cytokines in either ng/mL or U/mL concentrations in parallel.

**Table 2.** Cytokine concentrations applied for the differentiation of THP-1 cells into iDCs or mDCs, calculated by referring to the biological activity published by the manufacturer.

Cytokine	ng/mL	U/mL
GM-CSF	100 ng/mL	900 U/mL
[ImmunoTools, #1343125]	166.67 ng/mL	1500 U/mL
IL-4	100 ng/mL	2300 U/mL
[ImmunoTools, #11340045]	200 ng/mL	4600 U/mL
	65.22 ng/mL	1500 U/mL
	130.44 ng/mL	3000 U/mL
TNF- $\alpha$	20 ng/mL	400 U/mL
[PromoKine, #C-63719]	100 ng/mL	2000 U/mL

Differentiating THP-1 cells into iDCs in the presence of 100 ng/mL GM-CSF ( $\cong$ 900 U/mL) and 100 ng/mL IL-4 ( $\cong$ 2300 U/mL) resulted in a significantly higher number of cells expressing the surface markers CD54 (~95%), CD86 (~61%), and CD11b (~20%) (Figure 1A) compared to the undifferentiated control (CD54, ~58%; CD86, ~30%; CD11b, 3%). Furthermore, a pronounced higher geometric mean fluorescence intensity (GMFI) for HLA-DR (3.7-fold), CD54 (16.5-fold), and CD11b (3.1-fold) (Figure 1B) compared to the undifferentiated control could be detected. Supplementing the medium with 1500 U/mL GM-CSF and 1500 U/mL IL-4 induced the expression of CD54 (~88%), CD86 (~50%), and CD11b (~14%) on a significantly higher number of cells compared to the undifferentiated control (CD54, ~46%; CD86, ~24%; CD11b, ~3%) (Figure 1C) and a demonstrably higher GMFI for HLA-DR (4.1-fold), CD54 (14.6-fold), and CD11b (7.1-fold) (Figure 1D) compared to the undifferentiated control.

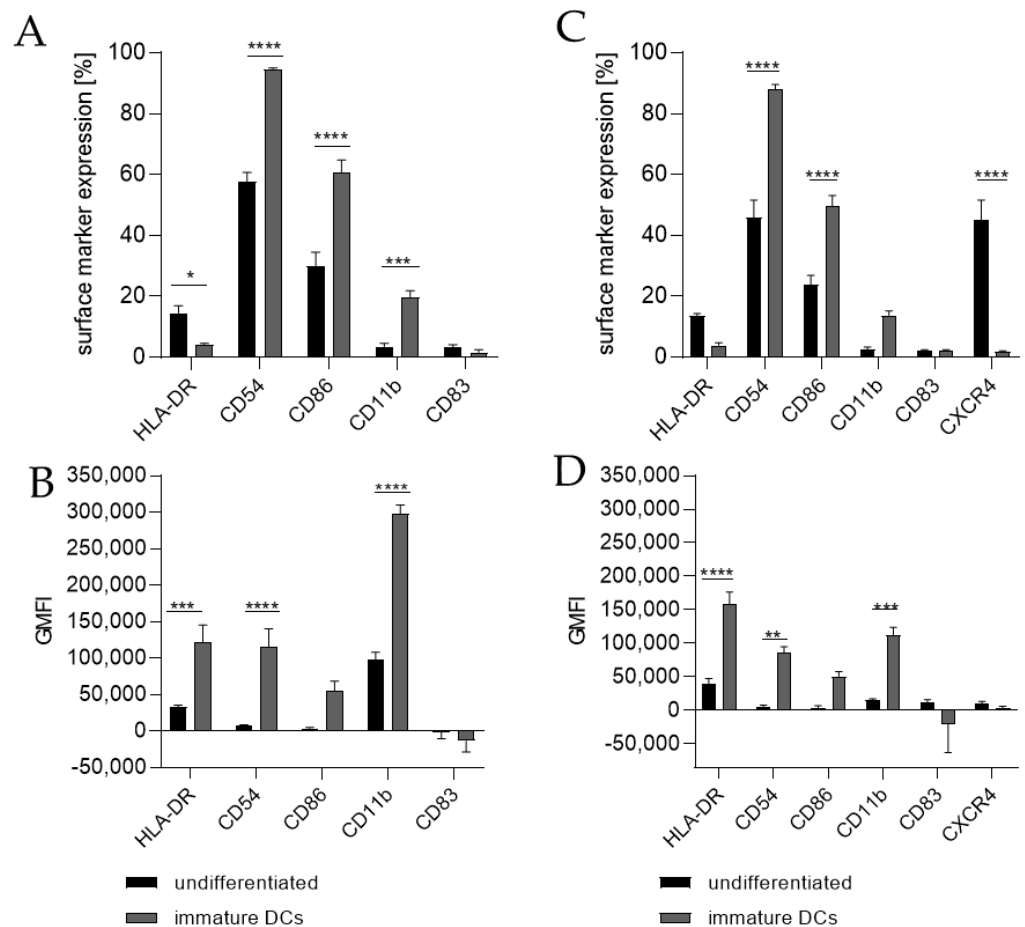


**Figure 1.** Surface marker expression of THP-1-derived iDCs, as follows: ng/mL (A,B) versus U/mL (C,D). Here,  $2 \times 10^5$  THP-1 cells/mL were seeded in 5 mL RPMI supplemented with 10% FBS, 1% PenStrep, and 0.05 mM 2-mercaptoethanol into a T25 flask. (A,B) For differentiation into iDCs, 100 ng/mL rhGM-CSF and 100 ng/mL rhIL-4 were added. (C,D) For differentiation into iDCs, 1500 U/mL rhGM-CSF and 1500 U/mL rhIL-4 were added. Cells were cultivated for 5 days, with medium exchange and addition of fresh cytokines after 72 h. Surface marker expression of at least 10,000 viable cells was analyzed via flow cytometry. Error bars indicate the standard errors of the mean ( $n = 3$  independent experiments with  $* = p \leq 0.05$ ,  $** = p \leq 0.01$ ,  $*** = p \leq 0.001$ , and  $**** = p \leq 0.0001$ ).

For the differentiation of THP-1 cells into mDCs, various protocols have been published. The main difference between those protocols is the direct differentiation of THP-1 cells into mDCs versus the differentiation of THP-1 cells into iDCs followed by further subsequent differentiation steps towards mDCs. Again, protocols using cytokine concentrations in ng/mL, as well as protocols based on concentrations in U/mL and various differentiation durations, have been published (Table 1).

Thus, we differentiated THP-1 in a one-step protocol into mDCs for 48 h with supplementation of 100 ng/mL GM-CSF ( $\cong 900$  U/mL), 200 ng/mL IL-4 ( $\cong 4600$  U/mL), 20 ng/mL ( $\cong 400$  U/mL) TNF- $\alpha$ , and 200 ng/mL ionomycin and with supplementation of 1500 U/mL GM-CSF, 3000 U/mL IL-4, 2000 U/mL TNF- $\alpha$ , and 200 ng/mL ionomycin for 48 h as well as for 72 h. The surface marker expression of mDCs generated from THP-1 cells cultivated in serum-free medium for 48 h was significantly higher for CD54 (ng/mL, ~100%; U/mL, ~99%), CD86 (ng/mL, ~73%; U/mL, ~73%), CD11b (ng/mL, ~44%; U/mL, ~52%), and CD83 (ng/mL, ~29%; U/mL, ~50%), but significantly lower for CXCR4 (ng/mL, ~2%; U/mL, ~3%) compared to the undifferentiated controls (CD54, ~75–77%; CD86, ~44–48%; CD11b, ~3–4%; CD83, 0%; CXCR4, 33–35%) (Figure 2A,C). The differentiation of THP-1 cells into mDCs for 72 h using U/mL concentrations led to significantly higher numbers of

cells expressing CD86 (~78%), CD11b (~49%), and CD83 (~35%), as well as CXCR4 (~70%), compared to the undifferentiated control (CD86, ~49%; CD11b, ~6%; CD83, ~0%; CXCR4, ~35%) (Figure 2E). Notably, a higher GMFI could only be observed for CD54 at a similar level (~ 415-fold) for all three differentiation approaches (Figure 2B,D,F).

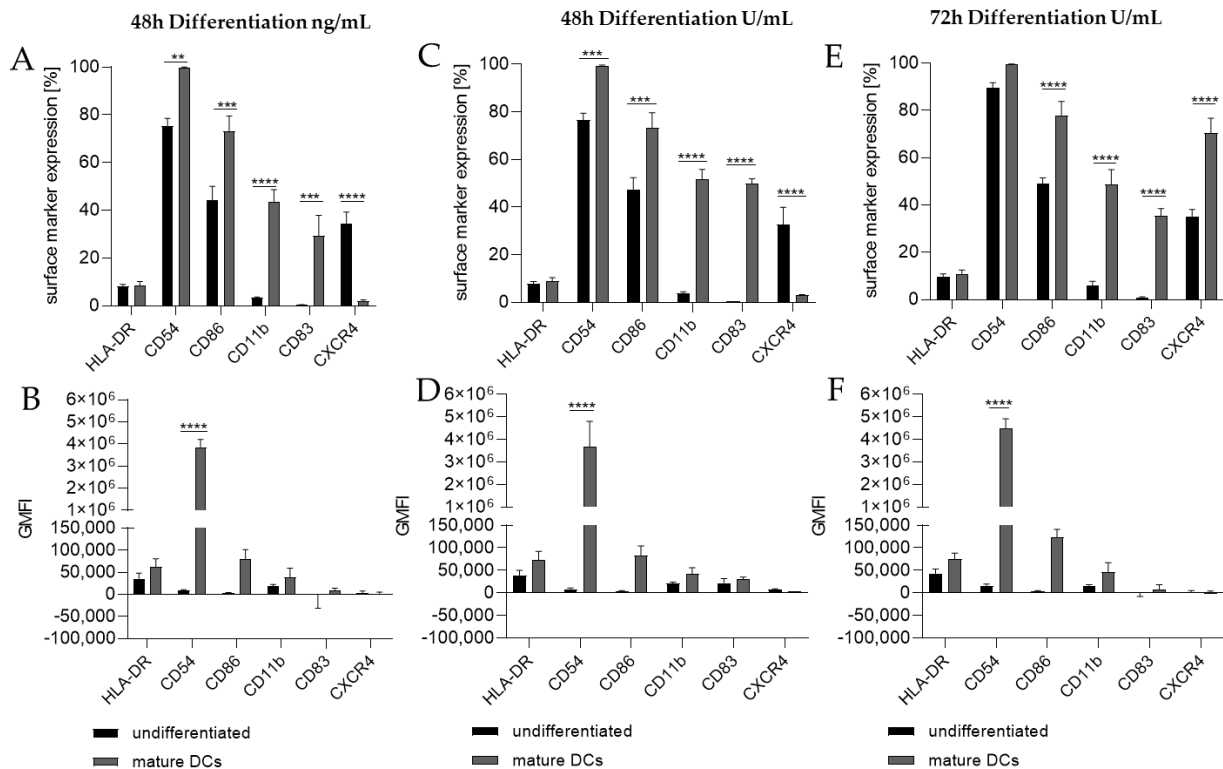


**Figure 2.** Surface marker expression of THP-1-derived mDCs, as follows: ng/mL (A,B) versus U/mL (C–F). Here,  $2 \times 10^5$  THP-1 cells/mL were seeded in 5 mL serum-free RPMI supplemented with 1% PenStrep, and 0.05 mM 2-mercaptoethanol into a T25 flask. (A,B) For differentiation into mDCs, 100 ng/mL rhGM-CSF, 200 ng/mL rhIL-4, 20 ng/mL TNF- $\alpha$ , and 200 ng/mL ionomycin were added. (C,D) For differentiation into mDCs, 1500 U/mL rhGM-CSF, 3000 U/mL rhIL-4, 2000 U/mL TNF- $\alpha$ , and 100 ng/mL ionomycin were added. Cells were cultivated for 48 h or 72 h. Surface marker expression of at least 10,000 viable cells was analyzed via flow cytometry. Error bars indicate the standard errors of the mean ( $n = 3$  independent experiments, with \*\* =  $p \leq 0.01$ , \*\*\* =  $p \leq 0.001$ , and \*\*\*\* =  $p \leq 0.0001$ ).

Since the morphology of mDCs could be differentiated between floating and adherent populations (Figure 3D), we also investigated the impact of a floating versus an adherent status on surface marker expression (Figure 4). Both floating and adherent mDCs expressed the surface markers CD54 (floating, ~99; adherent, ~98%), CD86 (floating, ~81; adherent, ~80%), and CD83 (floating, ~25; adherent, ~26%) at significantly higher rates than undifferentiated THP-1 cells (CD54, ~79%; CD86, ~41%; CD83, ~0%). Furthermore, although the numbers of cells expressing CXCR4 and CD11b was significantly higher on floating mDCs (CXCR4, ~46%; CD11b, ~29%), compared to undifferentiated THP-1 cells (CXCR4, ~20%; CD11b, ~3%), the surface marker expression of CXCR4 (~29%) and CD11b (~3%) on the adherent mDC population was not significantly higher compared to undifferentiated THP-1 cells (CXCR4, ~20%; CD11b, ~3%) (Figure 4A). However, significant changes in the GMFI for CD54 were detected for floating (273-fold) as well as for adherent (225-fold) mDCs. Although the number of cells expressing HLA-DR was not increased, the GMFI for floating cells was elevated (2.3-fold) and was even higher for adherent mDCs (5.8-fold) compared to the undifferentiated control (Figure 4B). Thus, the differentiation of THP-1 cells with GM-CSF, IL-4, TNF- $\alpha$ , and ionomycin leads to two different populations, namely floating

and adherent, which both reflect the marker expression of mature dendritic cells (CD54, CD86, and CD83), but display significant differences in CD11b and CXCR4 expression, which might be accompanied by different phagocytotic and migratory potential.

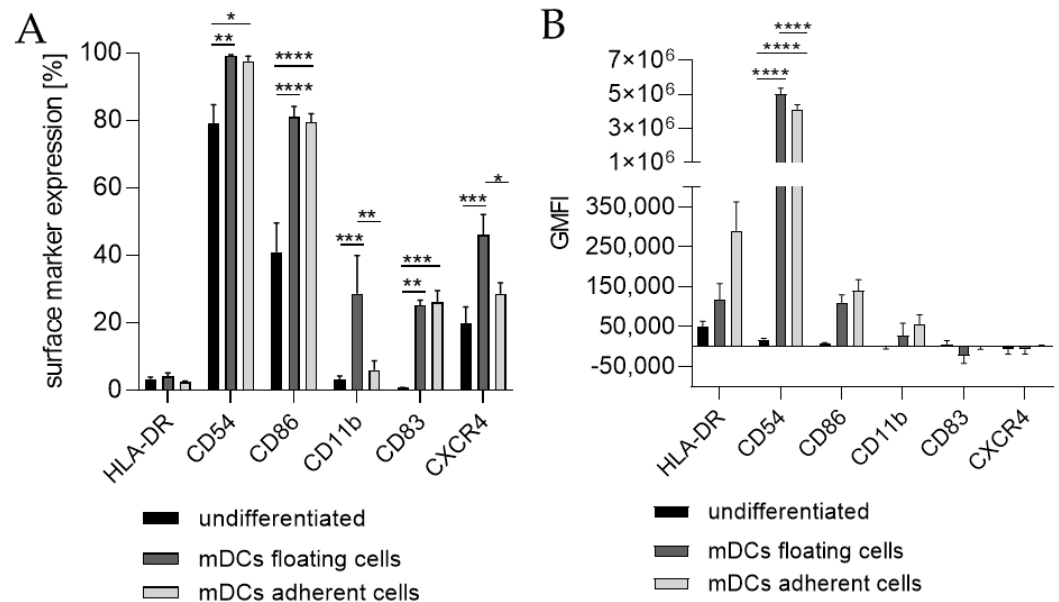


**Figure 3.** Surface marker expression of THP-1-derived mDCs. Floaters versus adherent cells. **(A)** Surface marker expression [%]. **(B)** Geometric mean fluorescence intensity (GMFI)  $2 \times 10^5$  THP-1 cells/mL were seeded in 20 mL serum-free RPMI supplemented with 1% PenStrep and 0.05 mM 2-mercaptoethanol into a T75 flask. For differentiation, 1500 U/mL rhGM-CSF, 3000 U/mL rIL-4, 2000 U/mL TNF- $\alpha$ , and 200 ng/mL ionomycin were added. Cells were cultivated for 72 h at 37 °C, 5% CO<sub>2</sub>. Surface marker expression of at least 10,000 viable cells was analyzed via flow cytometry. Error bars indicate the standard errors of the mean (n = 3 independent experiments with \* =  $p \leq 0.05$ ; \*\* =  $p \leq 0.01$ ; \*\*\* =  $p \leq 0.001$ ; and \*\*\*\* =  $p \leq 0.0001$ ).

Next, we differentiated THP-1-derived iDCs further into mDCs (Figure 5). The differentiation of iDCs into mDCs led to a significantly higher number of cells expressing CD54 (~99%), CD86 (~54%), and CD11b (~21%) compared to undifferentiated THP-1 cells (CD54, ~63%; CD86, ~33%; CD11b, ~2%). Notably, the CXCR4 expression was completely diminished. The number of cells expressing CD11b was significantly higher in iDCs (~27%) as well as in mDCs (~21%) compared to undifferentiated THP-1 cells (~2%), but lower in mDCs (~21%) compared to iDCs (~27%). Expression of CD83 on mDCs from THP-1-derived iDCs could not be induced (Figure 5A). The GMFI for CD54 was 29.8-fold induced on iDCs and 128-fold induced on iDC-derived mDCs. However, the GMFI for HLA-DR was increased at similar levels for iDCs (8.3-fold) and mDCs (8.0-fold), and the GMFI induction for CD86 was lower for mDCs (16.4-fold), than for iDCs (26.2-fold) (Figure 5B). Furthermore, the morphology of mDCs differentiated from THP-1-derived iDCs, as depicted in Figure 3F, reveals mainly loosely adherent cell clusters.

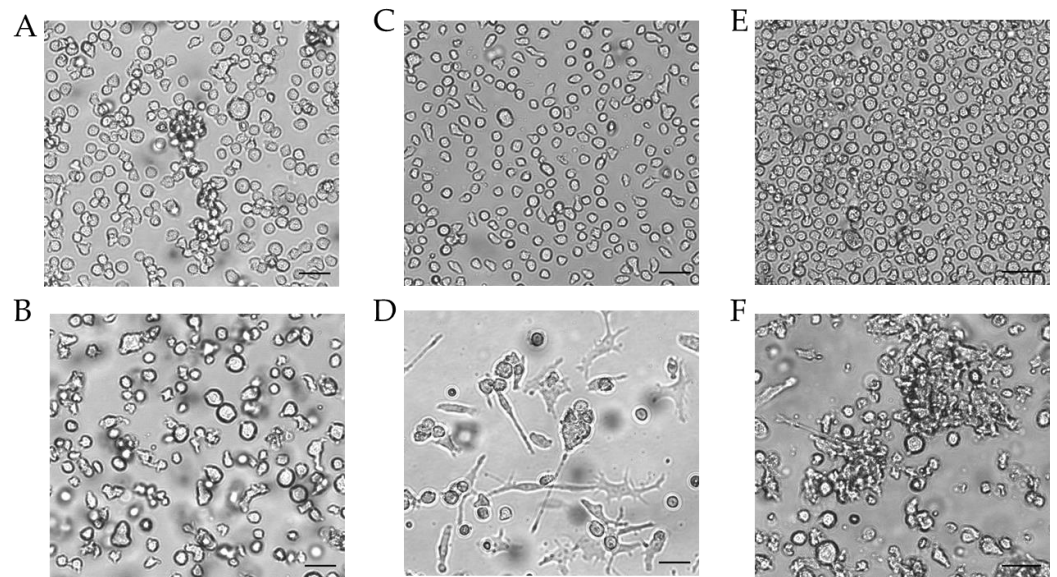


**Figure 4.** Morphology of THP-1-derived iDCs and mDCs using cytokine concentrations in U/mL. Morphology of undifferentiated THP-1 cells (A,C,E) according to the respective culture conditions of the differentiated cells. (B) Morphology of THP-1-derived immature dendritic cells (iDCs) (T25, U/mL, 5 d). (D) Morphology of THP-1-derived mDCs (T25, U/mL, 72 h). (F) Morphology of mDCs generated from THP-1-derived iDCs (T25, ng/mL, 48 h). Scale bar = 50  $\mu$ m.

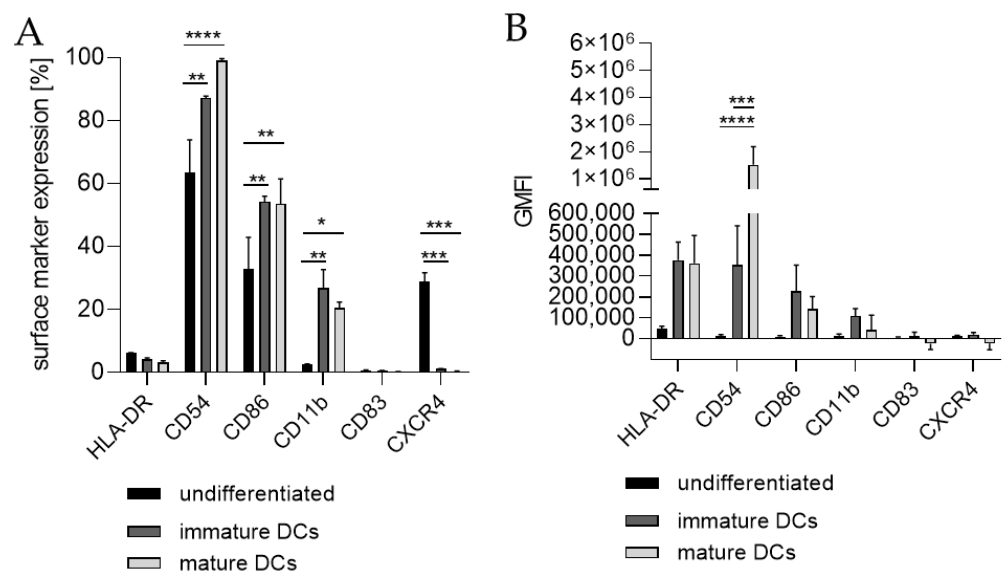


**Figure 5.** Surface marker expression of mDCs generated from-THP-1-derived iDCs. (A) Surface marker expression [%]. (B) Geometric mean fluorescence intensity (GMFI). Here,  $2 \times 10^5$  THP-1 cells/mL were seeded in 5 mL RPMI supplemented with 10% FBS, 1% PenStrep, and 0.05 mM 2-mercaptoethanol into a T25 flask and differentiated into iDCs (see Section 4.2). For further differentiation into mDCs, the medium was removed and fresh medium containing 100 ng/mL rhGM-CSF, 200 ng/mL rhIL-4, 20 ng/mL TNF- $\alpha$ , and 200 ng/mL ionomycin was added. Cells were cultivated for 48 h at 37  $^{\circ}$ C, 5% CO<sub>2</sub>. Surface marker expression of at least 10,000 viable cells was analyzed via flow cytometry. Error bars indicate the standard errors of the mean (n = 2 independent experiments with \* =  $p \leq 0.05$ , \*\* =  $p \leq 0.01$ , \*\*\* =  $p \leq 0.001$ , and \*\*\*\* =  $p \leq 0.0001$ ).

To investigate the ability of THP-1-derived iDCs to identify potential sensitizers, iDCs in comparison to undifferentiated THP-1 cells were treated for 24 h with either 20  $\mu$ M 1-chloro-2,4-dinitrobenzene (DNCB) or 380  $\mu$ M nickel sulfate (NiSO<sub>4</sub>), the defined positive

controls of the h-CLAT assay. As expected, the treatment of THP-1 cells with NiSO<sub>4</sub> led to a significantly higher expression of the h-CLAT key markers CD54 (~98%) and CD86 (~55%) and induced the expression of the maturation marker CD83 (~17%). Furthermore, treatment of iDCs with NiSO<sub>4</sub> resulted in a significant upregulation in CD54 (~97%), CD86 (~64%), and CXCR4 (~23%) (Figure 6A). The GMFI for CD54 was significantly higher (13.7-fold) after NiSO<sub>4</sub> treatment on THP-1 cells, but not as high as on iDCs after NiSO<sub>4</sub> treatment (29.2-fold) compared to untreated THP-1 cells. The GMFI for HLA-DR on iDCs was decreased after NiSO<sub>4</sub> treatment (1.5-fold), but not as much as on THP-1 cells with (6.4-fold) or without NiSO<sub>4</sub> treatment (5.6-fold) (Figure 6B). Furthermore, an increased GMFI (1.3-fold) for CD83 was observed after treatment of iDCs with NiSO<sub>4</sub>.

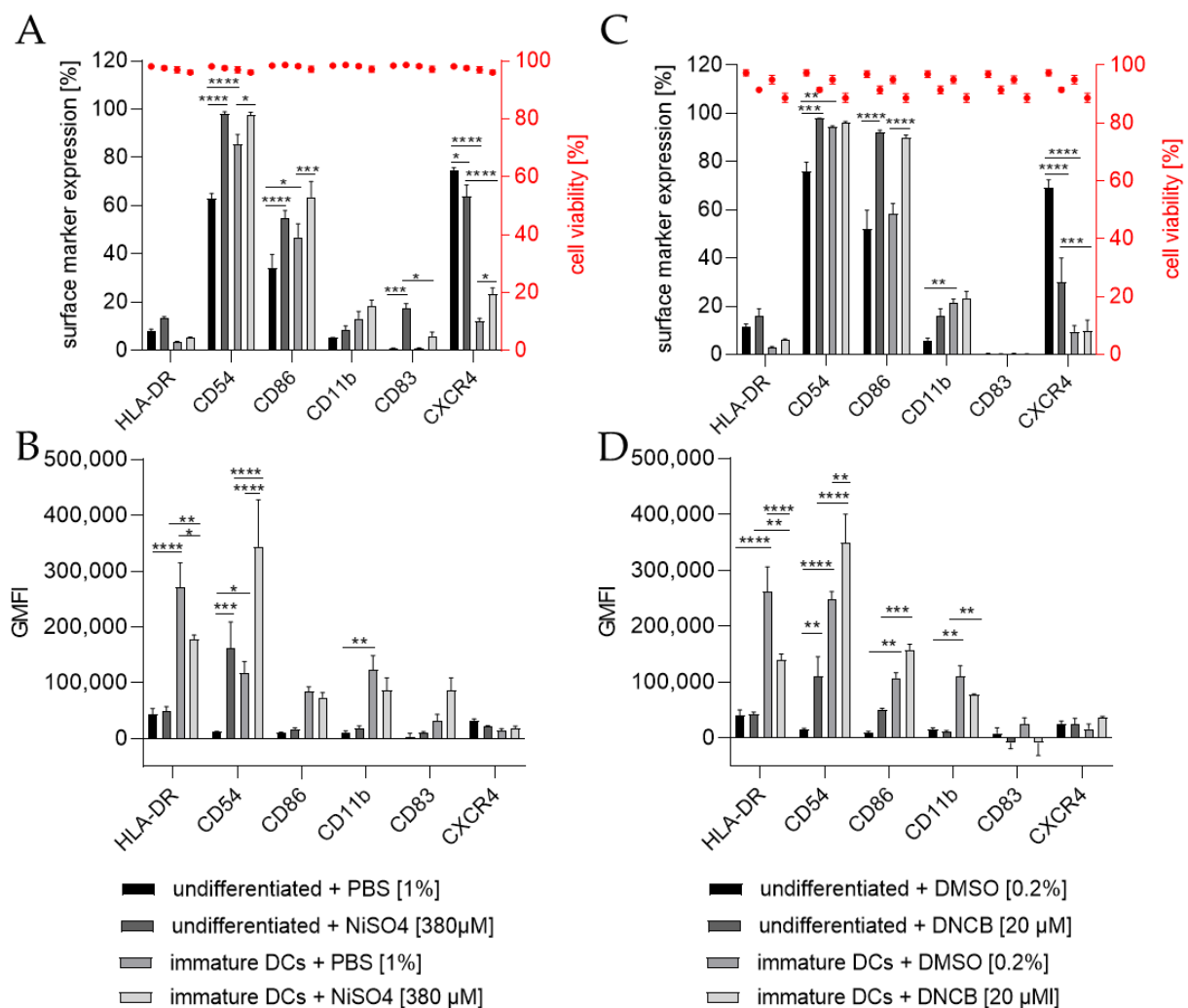


**Figure 6.** Surface marker expression of THP-1 cells or iDCs after sensitization according to the h-CLAT assay. (A,C) surface marker expression [%]. (B,D) Geometric mean fluorescence intensity (GMFI). Here, THP-1 cells or THP-1-derived iDCs (see Section 4.2) were seeded with  $1 \times 10^6$  cells/mL in 1 mL RPMI supplemented with 10% FBS, 1% PenStrep, and 0.05 mM 2-mercaptoethanol into a 24-well plate. Cells were treated with 20  $\mu$ M 1-Chloro-2,4-dinitrobenzene (DNCB) and 380  $\mu$ M nickel sulfate (NiSO<sub>4</sub>) or their respective solvent control, namely DMSO or PBS. Surface marker expression of at least 10,000 viable cells was analyzed via flow cytometry. Error bars indicate the standard errors of the mean ( $n = 3$  independent experiments with \* =  $p \leq 0.05$ , \*\* =  $p \leq 0.01$ , \*\*\* =  $p \leq 0.001$ , and \*\*\*\* =  $p \leq 0.0001$ ).

Treatment of THP-1 cells with 20  $\mu$ M DNCB also resulted in significantly more cells expressing the h-CLAT markers CD54 (~98%) and CD86 (~96%), but significantly fewer

cells expressing CXCR4 (~30%). Treatment of iDCs with DNCB resulted in significantly more cells expressing CD86 (~90%) (Figure 6C). Similar to the expression pattern of NiSO<sub>4</sub>-treated iDCs, treatment with DNCB led to a significantly higher GMFI for CD54 (3-fold) and lower GMFI for HLA-DR (1.9-fold) compared to untreated iDCs. However, compared to DNCB-treated THP-1 cells, the GMFI for HLA-DR is 3.3-fold higher, and the GMFI for CD11b is 7.2-fold higher on DNCB-treated iDCs (Figure 6D).

In order to prove the capability of our THP-1-derived DCs to phagocytose exogenous pathogen-derived particles, the DC surrogates were incubated with pHrodo Red-labeled zymosan, an insoluble  $\beta$ -1,3-glucan polysaccharide extracted from the cell wall of *Saccharomyces cerevisiae*. As pHrodo Red is a pH indicator dye, it is weakly fluorescent at neutral pH, but increases its fluorescence with decreasing pH during phagosomal acidification. As depicted in Figure 7 and as expected, significantly higher numbers of iDCs are able to phagocytose zymosan (~45%) compared to undifferentiated THP-1 cells (~17%) and to mDCs (~9%).

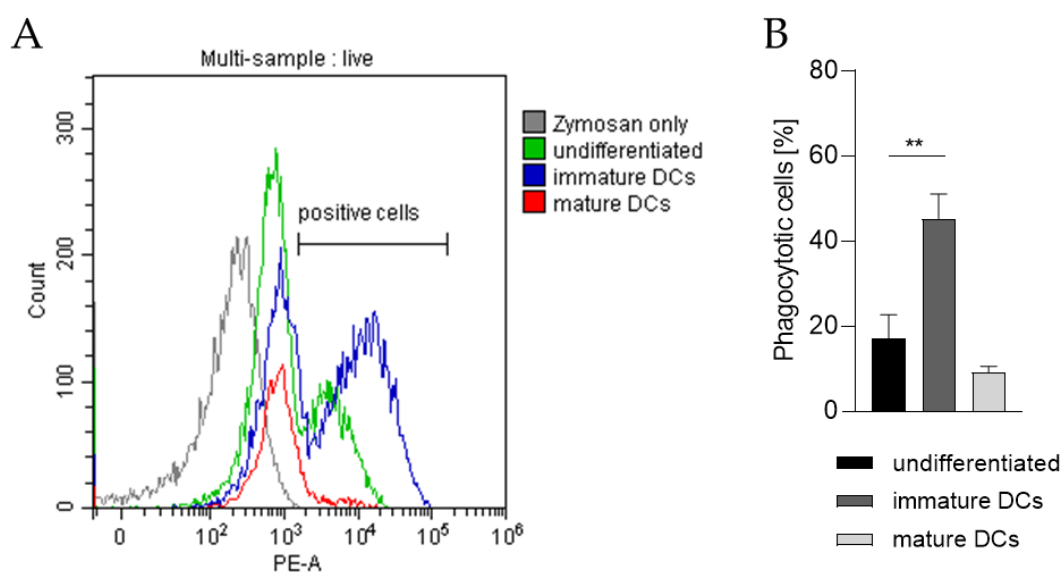


**Figure 7.** Phagocytotic capability of undifferentiated THP-1 cells, iDCs, and mDCs. Here, iDCs, as well as mDCs, were differentiated according to the U/mL protocols (see Sections 4.2 and 4.3). After 5 days and 72 h respectively,  $2 \times 10^5$  cells were resuspended in 100  $\mu$ L pHrodo Red zymosan bioparticles, seeded into 96-well plates, and cultivated for 1 h at 37  $^{\circ}$ C, 5% CO<sub>2</sub>. Then, DAPI was added before analysis of 10,000 living cells per sample via flow cytometry (Ex/Em, 560/585). (A) Gating strategy. (B) Number of cells (%) positive for phagocytosis. Error bars indicate the standard errors of the mean ( $n = 3$  independent experiments, with \*\* =  $p \leq 0.01$ ).

Moreover, the ability of iDCs to initiate T cell activation was investigated by analyzing the mRNA expression of the p40 chain of interleukin (IL)-12 via quantitative real-time PCR. For this, iDCs as well as undifferentiated THP-1 cells, were treated for 6 h with either 20  $\mu$ M DNCB or 380  $\mu$ M NiSO<sub>4</sub>, respectively. As expected, treatment of undifferentiated THP-1 cells with DNCB or NiSO<sub>4</sub> did not significantly alter the expression of IL-12p40 (Figure 8A). In contrast, mRNA expression of IL-12p40 was significantly higher in iDCs after DNCB treatment (4.5-fold), and 1.3-fold higher after NiSO<sub>4</sub> treatment, compared to the solvent control (Figure 8B), proving that differentiation of THP-1 cells into iDCs is required to study dendritic cell-mediated T cell activation.

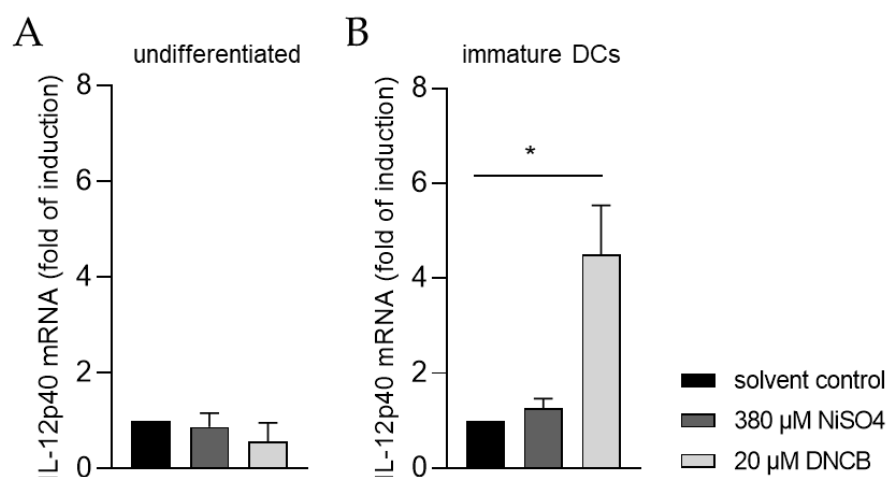


**Figure 8.** IL-12p40 mRNA expression of (A) THP-1 cells and (B) immature dendritic cells (iDCs) after sensitizer treatment. Here, THP-1 cells or THP-1-derived iDCs (see Section 4.2) were seeded with  $1 \times 10^6$  cells/mL in 1 mL RPMI supplemented with 10% FBS, 1% PenStrep, and 0.05 mM 2-mercaptoethanol into a 24-well plate. Cells were treated with 20  $\mu$ M DNCB or 380  $\mu$ M NiSO<sub>4</sub> for 6 h. Results were expressed as fold of induction compared to the solvent control and normalized to the expression of the housekeeping gene GAPDH. Error bars indicate the standard errors of the mean (n = 3 independent experiments with \* =  $p \leq 0.05$ ).

### 3. Discussion

The aim of this study was to generate robust, highly reproducible, and cost-effective protocols providing THP-1-derived iDC as well as mDC surrogates for in vitro human-based toxicological studies and for investigating the underlying mechanisms of sensitization and inflammation. In mediating the immune response, dendritic cells undergo various phenotypical changes, such as the upregulation of co-stimulatory molecules, maturation markers, and receptors regulating migratory behavior. In order to evaluate a conclusive differentiation of THP-1 cells into iDCs and mDCs as well as their potential for toxicological studies, we focused mainly on the DC activation markers CD54 and CD86, CD11b as marker for phagocytosis, the maturation marker CD83, and the migration marker CXCR4.

The differentiation of THP-1 cells into iDCs resulted in a significant upregulation in the surface markers CD54, CD86, and CD11b. The upregulation of CD54 together with CD86 are the key readout parameters of the h-CLAT aiming to mimic dendritic cell activation in order to predict skin sensitization [58,59]. Furthermore, co-stimulatory molecules, such as CD86, as well as CD80, often working in tandem, are upregulated during DC maturation, promoting CD 4<sup>+</sup> T cell activation [34,72]. The upregulation of CD86 as well as CD80 have been shown for THP-1-derived iDCs [62,64]. However, contrarily, Galbiati et al. described CD80 as well as CD86 expression below 15% on iDCs [65], not matching our results. It is known that CD11b plays an important role in phagocytosis [73], and its upregulation on THP-1-derived iDCs has been revealed by Czernek et al. [64], a study which confirms our data. Furthermore, HLA-DR is one of the MHC class II cell surface receptors, presenting the internalized and processed antigens to CD 4<sup>+</sup> T cells [74]. Even though our results displayed a low number of iDCs expressing HLA-DR, the GMFI for HLA-DR was significantly higher compared to undifferentiated cells, verifying an upregulation of HLA-DR molecules on HLA-DR-positive iDCs. This result matches the findings of Czernek et al., reporting a substantially higher MFI for HLA-DR on iDCs; unfortunately, Czernek et al. did not indicate the number of positive cells for HLA-DR [64]. However, as long as iDCs have not been exposed to antigens, MHC II molecules are retained by the invariant chain li in the late endosomal compartment [14]. In addition, it has been reported that only very few MHC II molecules are localized on the membrane of iDCs, and up to 75% of all MHC II molecules reside in the antigen processing compartments [15], confirming our results revealing low numbers of iDCs expressing HLA-DR on their surface. Furthermore, the differentiation

of THP-1 cells into iDCs did not induce the expression of CD83, a principal marker for cell maturation [75], matching the literature [62] and proving their immature status. To date, most protocols differentiating THP-1 cells into iDCs were performed in T75 flasks and 20 mL medium [62,65,66]. In contrast, we are the first to prove the differentiation of THP-1 cells into iDCs in T25 flasks, using 5 mL medium and, thus, only one quarter of the amount of the required cytokines, confirming our cost-effective approach.

For the generation of THP-1-derived mDCs, various protocols have been published, differentiating THP-1 cells directly into mDCs for 24 h [62], 48 h [62,66], 72 h [62], or generating mDCs from iDCs [63–65]. Differentiating THP-1 cells directly into mDCs for 48 h resulted in significantly higher numbers of cells expressing CD54, CD86, CD11b, and CD83, but a significantly lower (almost none) expression of CXCR4. Contrarily, the differentiation of THP-1 cells into mDCs for 72 h led to significantly enhanced numbers of CXCR4 expressing cells compared to the undifferentiated control. Furthermore, CXCR4 is one receptor for CXCL12/SDF-1, which is constitutively expressed and secreted in lymphoid tissues and other non-lymphoid tissues by bone marrow-, lymph node-, skin-, muscle-, and lung-derived fibroblasts, as well as by endothelial cells, liver and kidney cells, and the central nervous system [76–79]. Furthermore, various organs respond to tissue damage by increasing SDF-1 expression and secretion via hypoxia-inducible factor-1 (HIF-1) binding to the hypoxia-responsive region of the SDF-1 promotor [80]. Based on knockout studies or pharmacological blockade, CXCR4 has been proven to have a key role in DC differentiation [81], as well as in DC and Langerhans cell migration [23,24,82]. We are the first to prove CXCR4 expression on THP-1-derived mDCs. Coherent, upregulation of CXCR4 surface expression on mature dendritic cells has been shown for PBMC-derived dendritic cells [83] as well as for bone marrow-derived dendritic cells [84]. Furthermore, low CXCR4 mRNA levels for PBMC-derived iDCs and high CXCR4 levels for PBMC-derived mDCs have been detected by Sallusto et al. [21], confirming the CXCR4 expression pattern on our iDCs and mDCs. However, CXCR4 is not only expressed on mDCs, but also on naïve T cells and B lymphocytes [85], which may favor co-localization of those cells at sites where SDF-1 is secreted due to inflammation and tissue damage. Noteworthy, the direct differentiation of THP-1 cells into mDCs for 72 h led to two different subpopulations, namely floating and adherent cells. In both cell populations, CD83, the marker molecule for mature dendritic cells, was expressed by a similar quantity of cells, indicating no difference in maturation status. While the floating cells showed significantly higher expression of CXCR4 and CD11b than the undifferentiated THP-1 cells, the expression of CXCR4 and CD11b on adherent mDCs was only marginally higher than on undifferentiated THP-1 cells and significantly lower compared to the floating mDCs. Since CXCR4 is necessary for migration [23,24,82] and CD11b is involved in phagocytosis [73], it is coherent with the morphology and higher expression on floating cells which might be still in a steady state for the phagocytosis of antigens and migration to distinct sides. Furthermore, mDCs generated from THP-1-derived iDCs also display a different morphology compared to the mDCs which have been generated directly from THP-1 cells. While the directly generated mDCs were mostly strongly adherent and developed dendritic shaped branches, mDCs generated from iDCs formed loosely adherent cell clusters. Furthermore, CD11b expression was slightly lower than on iDCs and they expressed neither CD83 nor CXCR4. Based on these results we are confident that mDCs generated from THP-1-derived iDCs are not mDCs. Unfortunately, all publications which generated mDCs from THP-1-derived iDCs did not investigate the expression of CD83 or CXCR4, as successful maturation was assumed from high CD80 and CD86 expression [63–65]. Thus, only mDCs generated directly from THP-1 cells match the dendritic morphology and express the relevant maturation markers CD86 and CD83 as well as the migration marker CXCR4. However, for CXCR4 expression, it is mandatory to differentiate the THP-1 cells for 72 h and not as stated otherwise for 24 h or 48 h. Furthermore, comparing the differentiation results for iDCs and mDCs, expression levels for CD54, CD11b, and CD83 were different using cytokine concentrations indicated in ng/mL versus U/mL. Since the biological activity differs from supplier to supplier

and occasionally between lots, the indication of applied cytokine concentrations in U/mL is more precise and strongly advised for reproducible data. Complementary to the iDC protocols, most protocols for mDC generation were performed in T75 flasks in a volume of 20 mL medium. We are the first to prove differentiation of THP-1 cells into iDCs in T25 flasks, using 5 mL medium and, thus, only one quarter of the cytokines, thereby generating a cost-effective protocol.

As mentioned before, the upregulation of co-stimulatory molecules, as well as maturation markers in response to sensitizing and inflammation inducing agents, has become one of the key parameters to identify and predict the potential sensitizing and inflammatory capacity of substances. One of the most prominent assays is the h-CLAT, predicting sensitizers via CD54 and CD86 upregulation. The accuracy of the h-CLAT to distinguish sensitizers from non-sensitizers has been calculated as being between 76% and 83% [58,86,87]. In order to be classified as sensitizer, the relative fluorescence intensity (RFI) has to exceed a defined threshold, namely  $CD54 > 200$  or  $CD86 > 150$  [56,59]. However, detection of chemicals as false-negatives in the h-CLAT have been reported [54,87]. Our data reveals that the expression of CD54 as well as CD86, including percent positive cells and GMFI, is significantly higher for iDCs after sensitizer treatment compared to undifferentiated cells, which might allow a higher accuracy in detecting and subsequently categorizing sensitizers by decreasing rates of false-negative results and which might provide benefits for animal-free toxicological studies.

In order to demonstrate the functionality of our iDCs, their capability to phagocytose exogenous pathogen-derived particles as well as their potential to activate T cells was investigated. In their immature state, DCs are able to endocytose pathogens, which are further processed, initiating DC activation and maturation accompanied by the expression of surface markers, such as MHC II, CD54, and CD86. During the maturation process this ability decreases as DCs acquire primarily potent antigen presenting functions [12,88]. To assess the phagocytic potential of our DCs, cells were treated with zymosan, derived from the cell wall of *Saccharomyces cerevisiae*. While some undifferentiated THP-1 cells were able to phagocytose zymosan (17%), the number of phagocytotic iDCs was significantly higher (45%), whereas the number of mDCs phagocytosing zymosan decreased (9%). In line with our findings, high phagocytotic capability for iDCs has been reported for PBMC-derived as well as bone-marrow-derived iDCs [89–91]. Furthermore, lower phagocytotic capability of mDCs upon maturation has been shown for mDCs derived from PBMCs [91].

In order to activate naïve  $CD4^+$  T cells, DCs secrete IL-12, leading to upregulation of the transcription factor T-box expressed in T cells (T-bet) promoting their differentiation into interferon- $\gamma$  producing T helper 1 cells (Th1) [92,93]. Treatment of our THP-1-derived iDCs with DNCB resulted in significantly higher mRNA levels of IL-12p40 and in moderate higher mRNA levels of IL-12p40 in the presence of  $NiSO_4$ . Overall, we are able to demonstrate and prove the potential of THP-1-derived iDCs to induce T cell activation. Previous studies have shown IL-12p40 expression induction upon  $NiSO_4$  treatment of PBMC-derived iDCs [94,95], but not after DNCB treatment [94,96]. Contrarily, cutaneous treatment of mice with DNCB led to significantly enhanced IL-12p40 mRNA levels in local lymph nodes [97,98], as well as in spleens and the skin [99], tending to confirm our findings.

In conclusion, we were able to downscale the differentiation approaches by three-quarters, thereby generating robust, highly reproducible, and cost-effective protocols providing THP-1-derived iDC and mDC surrogates. The strong induction of CD54 as well as CD86 expression on iDCs after sensitizer treatment are applicable for in vitro toxicological studies, identifying potential sensitizing or inflammatory compounds and, in further steps, for assessing the anti-inflammatory potential of novel drug candidates. Based on the observed expression induction rates of CD11b, CD83, and CXCR4 as well as the IL-12p40 expression upon sensitizer treatment and the phagocytotic capability, our iDC and mDC surrogates are beneficial to study the molecular mechanisms of dendritic cell-mediated phagocytosis [73,100], dendritic cell maturation [101], as well as migration [22] and, furthermore, their use as therapeutic model systems in various disorders, such as sensitization,

inflammation [102,103], as well as cancer [104] and the tumor microenvironment [105], should not be discounted.

#### 4. Materials and Methods

##### 4.1. Cell Line Cultivation

The human monocytic leukemia cell line THP-1 (#TIB202, LOT:70025047) was purchased from ATCC (Manassas, VA, USA) (The THP-1 cells were maintained in T75 flasks (Greiner, #658195, Frickenhausen, Germany) in 20 mL RPMI (Gibco, #22400089, Grand Island, NY, USA) supplemented with 10% FBS (Gibco, #10270-106), 1% penicillin–streptomycin (PenStrep) (Gibco, #15140122), and 0.05 mM 2-mercaptoethanol (Gibco, #21985023) in a humidified incubator at 37 °C and 5% CO<sub>2</sub>. Cell density was maintained between  $1 \times 10^5$  cells/mL and  $5 \times 10^5$  cells/mL and cells were split every 2–3 days.

##### 4.2. Differentiation of THP-1 Cells into iDCs

For the generation of iDCs  $2 \times 10^5$  THP-1 cells/mL were seeded in 5 mL RPMI supplemented with 10% FBS, 1% PenStrep, and 0.05 mM 2-mercaptoethanol into a T25 flask. For differentiation, according to the published ng/mL concentrations, the following concentrations of cytokines were added: 100 ng/mL (=900 U/mL) rhGM-CSF (ImmunoTools, #11343125, Friesoythe, Germany), and 100 ng/mL (=2300 U/mL) rhIL-4 (ImmunoTools, #11340045). For differentiation using U/mL concentrations, 1500 IU/mL rhGM-CSF (ImmunoTools, #11343125) and 1500 IU/mL rhIL-4 (ImmunoTools, #11340045) were added. The cells were incubated for 5 days at 37 °C, 5% CO<sub>2</sub>, with medium exchange and addition of fresh cytokines on day 3.

##### 4.3. Differentiation of THP-1 Cells into mDCs

For differentiation of THP-1 cells into mDCs  $2 \times 10^5$  cells/mL in 5 mL or 20 mL serum-free RPMI supplemented with 1% PenStrep and 0.05 mM 2-mercaptoethanol was placed into a T25 flask or T75 flask. For differentiation according to ng/mL cytokine concentrations, the following concentrations were added: 100 ng/mL (=900 U/mL) rhGM-CSF (ImmunoTools, #11343125), 200 ng/mL (=4600 U/mL) rhIL-4 (ImmunoTools, #11340045), 20 ng/mL (=400 U/mL) TNF- $\alpha$  (PromoKine, #C63719), and 200 ng/mL ionomycin (Sigma-Aldrich, #I0634). For differentiation using U/mL concentrations, the following cytokines were added: 1500 IU/mL rhGM-CSF (ImmunoTools, #11343125), 3000 IU/mL rhIL-4 (ImmunoTools, #11340045), 2000 IU/mL TNF- $\alpha$  (PromoKine, #C63719, Heidelberg, Germany), and 200 ng/mL ionomycin (Sigma-Aldrich, #I0634, Darmstadt, Germany). The cells were cultivated for 48 h and 72 h at 37 °C, 5% CO<sub>2</sub>. For flow cytometry analysis, adherent cells were detached with accutase (Sigma-Aldrich, #A6964).

##### 4.4. Differentiation of THP-1-Derived iDCs into mDCs

The THP-1-derived iDCs were generated as stated in Section 4.2. On day 5, for further differentiation into mDCs, the medium was removed, and fresh medium containing 100 ng/mL (=900 U/mL) rhGM-CSF (ImmunoTools, #11343125), 200 ng/mL (=4600 U/mL) rhIL-4 (Immuno-Tools, #11340045), 20 ng/mL (=400 U/mL) TNF- $\alpha$  (PromoKine, #C63719), and 200 ng/mL ionomycin (Sigma-Aldrich, #I0634) was added. The cells were cultivated for 48 h at 37 °C, 5% CO<sub>2</sub>. For flow cytometry analysis, adherent cells were detached with accutase (Sigma-Aldrich, #A6964).

##### 4.5. Sensitization Assay According to the h-CLAT

The THP-1 cells or THP-1-derived iDCs (see Section 4.2) were seeded and treated accordingly to the h-CLAT assay. Briefly,  $1 \times 10^6$  cells/mL were seeded in 1 mL RPMI supplemented with 10% FBS, 1% PenStrep, and 0.05 mM 2-mercaptoethanol into a 24-well plate. Cells were treated with 20  $\mu$ M 1-chloro-2,4-dinitrobenzene (DNCB) (Sigma-Aldrich, #237329, Darmstadt, Germany) and 380  $\mu$ M nickel sulfate (NiSO<sub>4</sub>) (Sigma-Aldrich, #227676) or their respective solvent control, namely dimethylsulfoxide (DMSO) or Dulbecco's phos-

phate buffered saline (PBS). After 24 h, the cells were harvested, and surface marker expression was determined via flow cytometry (see Section 4.6).

#### 4.6. Surface Marker Detection via Flow Cytometry

Cells were harvested after differentiation and washed thrice in autoMACS running buffer (Miltenyi Biotec, #130-091-221, Gladbach, Germany). Cells were transferred to 96-well plates with  $2 \times 10^5$  cells for each antibody panel. Cells were stained with the following antibodies: diluted 1:50, REA Control (S)-VioGreen (Miltenyi Biotec, #130-113-444), REA Control (S)-PE (Miltenyi Biotec, #130-113-438), REA Control (S)-APC (Miltenyi Biotec, #130-113-434); REA Control (S)-PE-Vio770, (Miltenyi Biotec, #130-113-440); HLA-DR-VioGreen (Miltenyi Biotec, #130-111-795), CD54-APC (Miltenyi Biotec, #130-121-342); CXCR4-PE-Vio770 (Miltenyi Biotec, #130-116-161); CD11b-VioGreen (Miltenyi Biotec, #130-110-617); CD83-PE (Miltenyi Biotec, #130-110-561); CD86-APC (Miltenyi Biotec, #130-116-161) for 10 min at 4 °C in the dark. Afterwards, cells were washed thrice with autoMACS running buffer and stained with DAPI (Sigma, #D9542), to exclude dead cells for the determination of the cell viability.

#### 4.7. Phagocytosis Assay

Phagocytosis assays were performed using pHrodo red zymosan particles (Invitrogen™, #P35364, Waltham, MA, USA), dissolved in RPMI supplemented with 10% FBS, 1% PenStrep, and 0.05 mM 2-mercaptoethanol at a concentration of 0.5 mg/mL. Cells were harvested after differentiation and  $2 \times 10^5$  cells were resuspended in 100 µL pHrodo red zymosan particles and seeded into 96-well plates. The cells were cultivated for 1 h at 37 °C, 5% CO<sub>2</sub>. Then, DAPI was added before the analysis of 10,000 living cells per sample via flow cytometry (Ex/Em, 560/585).

#### 4.8. Analysis of IL-12p40 mRNA Expression by Quantitative Real-Time PCR

The THP-1 cells or THP-1-derived iDCs (see Section 4.2) were seeded and treated according to the h-CLAT assay. Briefly,  $1 \times 10^6$  cells/mL were seeded in 1 mL RPMI supplemented with 10% FBS, 1% PenStrep, and 0.05 mM 2-mercaptoethanol into a 24-well plate. Cells were treated with 20 µM 1-chloro-2,4-dinitrobenzene (DNCB) (Sigma-Aldrich, #237329) and 380 µM nickel sulfate (NiSO<sub>4</sub>) (Sigma-Aldrich, #227676) or their respective solvent control, namely dimethylsulfoxide (DMSO) or Dulbecco's phosphate buffered saline (PBS) for 6 h. Total RNA was extracted according to the manufacturer's instructions using the RNeasy MiniKit (Qiagen, #74104, Hilden, Germany). The RNA concentration was determined by OD<sub>260/280</sub> measurement using the Tecan Spark NanoQuant Plate. A total of 1 µg of RNA was reverse transcribed using the QuatiTect Reverse Transcription Kit (Qiagen, #205311). Quantitative real-time PCR (qPCR) reactions were performed for 50 ng cDNA in triplicate for each sample on a qTower<sup>3</sup> G (Analytikjena, Jena, Germany), using Luna Universal qPCR Master Mix (NEB, #M3003L, Ipswich, MA, USA). The specific primers used were GAPDH (forward, 5'-TGCACCACCAACTGCTTAGC-3'; reverse, 5'-GGCATGGACTGTGGTCATGAG-3') and IL-12p40 (forward, 5'-TGTCGTAGAATTGGATTGGTATC-3'; reverse, 5'-AACCT GCCTCCTTTGTG-3'). After amplification, a threshold was set for each gene and Ct values were calculated for all samples.

#### 4.9. Statistical Analysis

Statistical analysis was performed using GraphPad Prism version 8.4.3 (GraphPad Software, Inc., San Diego, CA, USA). Statistical significance was determined using two-way ANOVA, Sidak's multiple comparisons test or Tukey's multiple comparisons test. Significance was defined as \* =  $p \leq 0.05$ ; \*\* =  $p \leq 0.01$ ; \*\*\* =  $p \leq 0.001$ ; \*\*\*\* =  $p \leq 0.0001$ .

**Author Contributions:** Conceptualization, N.T.; methodology, J.M.H.; software, J.M.H.; validation, J.M.H.; formal analysis, J.M.H.; investigation, J.M.H.; resources, N.T.; data curation, J.M.H.; writing—original draft preparation, J.M.H.; writing—review and editing, N.T. and J.M.H.; visualization, J.M.H.;

supervision, N.T. project administration, N.T.; funding acquisition, N.T. All authors have read and agreed to the published version of the manuscript.

**Funding:** This research was funded by a grant to N.T. by the Bundesministerium für Ernährung und Landwirtschaft (BMEL), funding number: 281A308C18.

**Institutional Review Board Statement:** Not applicable.

**Informed Consent Statement:** Not applicable.

**Data Availability Statement:** Not applicable.

**Acknowledgments:** The authors would like to thank Ursula Engels for sharing her profound knowledge regarding the h-CLAT assay and Kira Ludwig for her technical assistance.

**Conflicts of Interest:** The authors declare no conflict of interest. The funders had no role in the design of the study; in the collection, analyses, or interpretation of data; in the writing of the manuscript; or in the decision to publish the results.

## References

1. Eidsmo, L.; Allan, R.; Caminschi, I.; van Rooijen, N.; Heath, W.R.; Carbone, F.R. Differential migration of epidermal and dermal dendritic cells during skin infection. *J. Immunol.* **2009**, *182*, 3165–3172. [[CrossRef](#)] [[PubMed](#)]
2. e Sousa, C.R. Dendritic cells as sensors of infection. *Immunity* **2001**, *14*, 495–498. [[CrossRef](#)] [[PubMed](#)]
3. Liu, J.; Zhang, X.; Cheng, Y.; Cao, X. Dendritic cell migration in inflammation and immunity. *Cell. Mol. Immunol.* **2021**, *18*, 2461–2471. [[CrossRef](#)] [[PubMed](#)]
4. Hardonnière, K.; Szely, N.; El Ali, Z.; Pallardy, M.; Kerdine-Römer, S. Models of Dendritic Cells to Assess Skin Sensitization. *Front. Toxicol.* **2022**, *4*, 851017. [[CrossRef](#)] [[PubMed](#)]
5. Liu, L.; Watanabe, M.; Minami, N.; Yunizar, M.F.; Ichikawa, T. Dendritic Cells Directly Recognize Nickel Ions as an Antigen during the Development of Nickel Allergy. *J. Oral Health Biosci.* **2022**, *34*, 40–52.
6. Vella, J.L.; Molodtsov, A.; Angeles, C.V.; Branchini, B.R.; Turk, M.J.; Huang, Y.H. Dendritic cells maintain anti-tumor immunity by positioning CD8 skin-resident memory T cells. *Life Sci. Alliance* **2021**, *4*. [[CrossRef](#)]
7. Zhou, L.; Jiang, A.; Veenstra, J.; Ozog, D.M.; Mi, Q.-S. The Roles of Skin Langerhans Cells in Immune Tolerance and Cancer Immunity. *Vaccines* **2022**, *10*, 1380. [[CrossRef](#)]
8. Hölken, J.M.; Teusch, N.E. Recent developments of 3D models of the tumor microenvironment for cutaneous melanoma: Bridging the gap between the bench and the bedside? *J. Transl. Sci.* **2020**, *7*, 1–7.
9. Steinman, R.M.; Banchereau, J. Taking dendritic cells into medicine. *Nature* **2007**, *449*, 419–426. [[CrossRef](#)]
10. Collin, M.; Bigley, V. Human dendritic cell subsets: An update. *Immunology* **2018**, *154*, 3–20. [[CrossRef](#)]
11. Guillemins, M.; Ginhoux, F.; Jakubzick, C.; Naik, S.H.; Onai, N.; Schraml, B.U.; Segura, E.; Tussiwand, R.; Yona, S. Dendritic cells, monocytes and macrophages: A unified nomenclature based on ontogeny. *Nat. Rev. Immunol.* **2014**, *14*, 571–578. [[CrossRef](#)] [[PubMed](#)]
12. Liu, Z.; Roche, P.A. Macropinocytosis in phagocytes: Regulation of MHC class-II-restricted antigen presentation in dendritic cells. *Front. Physiol.* **2015**, *6*, 1. [[CrossRef](#)] [[PubMed](#)]
13. Wilson, N.S.; El-Sukkari, D.; Villadangos, J.A. Dendritic cells constitutively present self antigens in their immature state in vivo and regulate antigen presentation by controlling the rates of MHC class II synthesis and endocytosis. *Blood* **2004**, *103*, 2187–2195. [[CrossRef](#)] [[PubMed](#)]
14. Neefjes, J.; Jongstra, M.L.M.; Paul, P.; Bakke, O. Towards a systems understanding of MHC class I and MHC class II antigen presentation. *Nat. Rev. Immunol.* **2011**, *11*, 823–836. [[CrossRef](#)] [[PubMed](#)]
15. Roche, P.A.; Furuta, K. The ins and outs of MHC class II-mediated antigen processing and presentation. *Nat. Rev. Immunol.* **2015**, *15*, 203–216. [[CrossRef](#)]
16. Klein, J.; Sato, A. The HLA system. *N. Engl. J. Med.* **2000**, *343*, 702–709. [[CrossRef](#)]
17. Embgenbroich, M.; Burgdorf, S. Current Concepts of Antigen Cross-Presentation. *Front. Immunol.* **2018**, *9*, 01643. [[CrossRef](#)]
18. Joffre, O.P.; Segura, E.; Savina, A.; Amigorena, S. Cross-presentation by dendritic cells. *Nat. Rev. Immunol.* **2012**, *12*, 557–569. [[CrossRef](#)]
19. Granucci, F.; Ferrero, E.; Foti, M.; Aggujaro, D.; Vettoretto, K.; Ricciardi-Castagnoli, P. Early events in dendritic cell maturation induced by LPS. *Microb. Infect.* **1999**, *1*, 1079–1084. [[CrossRef](#)]
20. Toebak, M.J.; Gibbs, S.; Bruynzeel, D.P.; Scheper, R.J.; Rustemeyer, T. Dendritic cells: Biology of the skin. *Contact Dermat.* **2009**, *60*, 2–20. [[CrossRef](#)]
21. Sallusto, F.; Schaerli, P.; Loetscher, P.; Schaniel, C.; Lenig, D.; Mackay, C.R.; Qin, S.; Lanzavecchia, A. Rapid and coordinated switch in chemokine receptor expression during dendritic cell maturation. *Eur. J. Immunol.* **1998**, *28*, 2760–2769. [[CrossRef](#)]
22. Tiberio, L.; Del Prete, A.; Schioppa, T.; Sozio, F.; Bosisio, D.; Sozzani, S. Chemokine and chemotactic signals in dendritic cell migration. *Cell Mol. Immunol.* **2018**, *15*, 346–352. [[CrossRef](#)] [[PubMed](#)]

23. Kabashima, K.; Shiraishi, N.; Sugita, K.; Mori, T.; Onoue, A.; Kobayashi, M.; Sakabe, J.; Yoshiki, R.; Tamamura, H.; Fujii, N.; et al. CXCL12-CXCR4 engagement is required for migration of cutaneous dendritic cells. *Am. J. Pathol.* **2007**, *171*, 1249–1257. [[CrossRef](#)] [[PubMed](#)]
24. Ouwehand, K.; Santegoets, S.J.; Bruynzeel, D.P.; Scheper, R.J.; de Gruijl, T.D.; Gibbs, S. CXCL12 is essential for migration of activated Langerhans cells from epidermis to dermis. *Eur. J. Immunol.* **2008**, *38*, 3050–3059. [[CrossRef](#)]
25. Förster, R.; Schubel, A.; Breitfeld, D.; Kremmer, E.; Renner-Müller, I.; Wolf, E.; Lipp, M. CCR7 coordinates the primary immune response by establishing functional microenvironments in secondary lymphoid organs. *Cell* **1999**, *99*, 23–33. [[CrossRef](#)]
26. Saeki, H.; Moore, A.M.; Brown, M.J.; Hwang, S.T. Cutting edge: Secondary lymphoid-tissue chemokine (SLC) and CC chemokine receptor 7 (CCR7) participate in the emigration pathway of mature dendritic cells from the skin to regional lymph nodes. *J. Immunol.* **1999**, *162*, 2472–2475. [[CrossRef](#)]
27. Braun, A.; Worbs, T.; Moschovakis, G.L.; Halle, S.; Hoffmann, K.; Bölder, J.; Münk, A.; Förster, R. Afferent lymph–derived T cells and DCs use different chemokine receptor CCR7–dependent routes for entry into the lymph node and intranodal migration. *Nat. Immunol.* **2011**, *12*, 879–887. [[CrossRef](#)]
28. La Gruta, N.L.; Gras, S.; Daley, S.R.; Thomas, P.G.; Rossjohn, J. Understanding the drivers of MHC restriction of T cell receptors. *Nat. Rev. Immunol.* **2018**, *18*, 467–478. [[CrossRef](#)]
29. Tai, Y.; Wang, Q.; Korner, H.; Zhang, L.; Wei, W. Molecular mechanisms of T cells activation by dendritic cells in autoimmune diseases. *Front. Pharmacol.* **2018**, *9*, 642. [[CrossRef](#)]
30. Lim, T.S.; Goh, J.K.H.; Mortellaro, A.; Lim, C.T.; Hämmerling, G.J.; Ricciardi-Castagnoli, P. CD80 and CD86 Differentially Regulate Mechanical Interactions of T-Cells with Antigen-Presenting Dendritic Cells and B-Cells. *PLoS ONE* **2012**, *7*, e45185. [[CrossRef](#)]
31. Parameswaran, N.; Suresh, R.; Bal, V.; Rath, S.; George, A. Lack of ICAM-1 on APCs during T Cell Priming Leads to Poor Generation of Central Memory Cells. *J. Immunol.* **2005**, *175*, 2201. [[CrossRef](#)] [[PubMed](#)]
32. Dustin, M.L.; Tseng, S.-Y.; Varma, R.; Campi, G. T cell–dendritic cell immunological synapses. *Curr. Opin. Immunol.* **2006**, *18*, 512–516. [[CrossRef](#)] [[PubMed](#)]
33. Leithner, A.; Altenburger, L.M.; Hauschild, R.; Assen, F.P.; Rottner, K.; Stradal, T.E.B.; Diz-Muñoz, A.; Stein, J.V.; Sixt, M. Dendritic cell actin dynamics control contact duration and priming efficiency at the immunological synapse. *J. Cell Biol.* **2021**, *220*. [[CrossRef](#)]
34. Dolatkhan, K.; Alizadeh, N.; Mohajjel-Shoja, H.; Shadbad, M.A.; Hajiasgharzadeh, K.; Aghebati-Maleki, L.; Baghbanzadeh, A.; Hosseinkhani, N.; Ahangar, N.K.; Baradaran, B. B7 immune checkpoint family members as putative therapeutics in autoimmune disease: An updated overview. *Int. J. Rheum. Dis.* **2022**, *25*, 259–271. [[CrossRef](#)] [[PubMed](#)]
35. Sharpe, A.H.; Freeman, G.J. The B7–CD28 superfamily. *Nat. Rev. Immunol.* **2002**, *2*, 116–126. [[CrossRef](#)] [[PubMed](#)]
36. Lanzavecchia, A.; Sallusto, F. Regulation of T cell immunity by dendritic cells. *Cell* **2001**, *106*, 263–266. [[CrossRef](#)]
37. Klein, E.; Koch, S.; Borm, B.; Neumann, J.; Herzog, V.; Koch, N.; Bieber, T. CD83 localization in a recycling compartment of immature human monocyte-derived dendritic cells. *Int. Immunol.* **2005**, *17*, 477–487. [[CrossRef](#)]
38. Cao, W.; Lee, S.H.; Lu, J. CD83 is preformed inside monocytes, macrophages and dendritic cells, but it is only stably expressed on activated dendritic cells. *Biochem. J.* **2005**, *385*, 85–93. [[CrossRef](#)]
39. Fujimoto, Y.; Tu, L.; Miller, A.S.; Bock, C.; Fujimoto, M.; Doyle, C.; Steeber, D.A.; Tedder, T.F. CD83 expression influences CD4+ T cell development in the thymus. *Cell* **2002**, *108*, 755–767. [[CrossRef](#)]
40. Doebbler, M.; Koenig, C.; Krzyzak, L.; Seitz, C.; Wild, A.; Ulas, T.; Baßler, K.; Kopelyanskiy, D.; Butterhof, A.; Kuhnt, C.; et al. CD83 expression is essential for Treg cell differentiation and stability. *JCI Insight* **2018**, *3*. [[CrossRef](#)]
41. von Rohrscheidt, J.; Petrozziello, E.; Nedjic, J.; Federle, C.; Krzyzak, L.; Ploegh, H.L.; Ishido, S.; Steinkasserer, A.; Klein, L. Thymic CD4 T cell selection requires attenuation of MARCH8-mediated MHCII turnover in cortical epithelial cells through CD83. *J. Exp. Med.* **2016**, *213*, 1685–1694. [[CrossRef](#)]
42. Walseng, E.; Bandola-Simon, J.; Roche, P. The role of transmembrane domains in the MARCH-I-mediated downregulation of MHC-II and CD86. *J. Immunol.* **2017**, *198*, 146. [[CrossRef](#)]
43. Tze, L.E.; Horikawa, K.; Domaschensz, H.; Howard, D.R.; Roots, C.M.; Rigby, R.J.; Way, D.A.; Ohmura-Hoshino, M.; Ishido, S.; Andoniou, C.E.; et al. CD83 increases MHC II and CD86 on dendritic cells by opposing IL-10-driven MARCH1-mediated ubiquitination and degradation. *J. Exp. Med.* **2011**, *208*, 149–165. [[CrossRef](#)]
44. Bouso, P. T-cell activation by dendritic cells in the lymph node: Lessons from the movies. *Nat. Rev. Immunol.* **2008**, *8*, 675–684. [[CrossRef](#)] [[PubMed](#)]
45. Pasparakis, M.; Haase, I.; Nestle, F.O. Mechanisms regulating skin immunity and inflammation. *Nat. Rev. Immunol.* **2014**, *14*, 289–301. [[CrossRef](#)] [[PubMed](#)]
46. Basketter, D.A.; Kimber, I. Skin sensitization, false positives and false negatives: Experience with guinea pig assays. *J. Appl. Toxicol.* **2010**, *30*, 381–386. [[CrossRef](#)]
47. Coutant, K.D.; de Fraissinette, A.B.; Cordier, A.; Ulrich, P. Modulation of the activity of human monocyte-derived dendritic cells by chemical haptens, a metal allergen, and a staphylococcal superantigen. *Toxicol. Sci.* **1999**, *52*, 189–198. [[CrossRef](#)]
48. Kiertcher, S.M.; Roth, M.D. Human CD14+ leukocytes acquire the phenotype and function of antigen-presenting dendritic cells when cultured in GM-CSF and IL-4. *J. Leukoc. Biol.* **1996**, *59*, 208–218. [[CrossRef](#)]
49. Palucka, K.A.; Taquet, N.; Sanchez-Chapuis, F.; Gluckman, J.C. Dendritic cells as the terminal stage of monocyte differentiation. *J. Immunol.* **1998**, *160*, 4587–4595. [[CrossRef](#)]

50. Chapuis, F.; Rosenzweig, M.; Yagello, M.; Ekman, M.; Biberfeld, P.; Gluckman, J.C. Differentiation of human dendritic cells from monocytes in vitro. *Eur. J. Immunol.* **1997**, *27*, 431–441. [[CrossRef](#)]
51. Chanput, W.; Mes, J.J.; Wichers, H.J. THP-1 cell line: An in vitro cell model for immune modulation approach. *Int. Immunopharmacol.* **2014**, *23*, 37–45. [[CrossRef](#)] [[PubMed](#)]
52. Aiba, S.; Terunuma, A.; Manome, H.; Tagami, H. Dendritic cells differently respond to haptens and irritants by their production of cytokines and expression of co-stimulatory molecules. *Eur. J. Immunol.* **1997**, *27*, 3031–3038. [[CrossRef](#)] [[PubMed](#)]
53. Ashikaga, T.; Yoshida, Y.; Hirota, M.; Yoneyama, K.; Itagaki, H.; Sakaguchi, H.; Miyazawa, M.; Ito, Y.; Suzuki, H.; Toyoda, H. Development of an in vitro skin sensitization test using human cell lines: The human Cell Line Activation Test (h-CLAT): I. Optimization of the h-CLAT protocol. *Toxicol. Vitro.* **2006**, *20*, 767–773. [[CrossRef](#)] [[PubMed](#)]
54. Ashikaga, T.; Sakaguchi, H.; Sono, S.; Kosaka, N.; Ishikawa, M.; Nukada, Y.; Miyazawa, M.; Ito, Y.; Nishiyama, N.; Itagaki, H. A Comparative Evaluation of In Vitro Skin Sensitisation Tests: The Human Cell-line Activation Test (h-CLAT) versus the Local Lymph Node Assay (LLNA). *Altern. Lab. Anim.* **2010**, *38*, 275–284. [[CrossRef](#)] [[PubMed](#)]
55. Tsuchiya, S.; Yamabe, M.; Yamaguchi, Y.; Kobayashi, Y.; Konno, T.; Tada, K. Establishment and characterization of a human acute monocytic leukemia cell line (THP-1). *Int. J. Cancer* **1980**, *26*, 171–176. [[CrossRef](#)]
56. Sakaguchi, H.; Ashikaga, T.; Miyazawa, M.; Kosaka, N.; Ito, Y.; Yoneyama, K.; Sono, S.; Itagaki, H.; Toyoda, H.; Suzuki, H. The relationship between CD86/CD54 expression and THP-1 cell viability in an in vitro skin sensitization test–human cell line activation test (h-CLAT). *Cell Biol. Toxicol.* **2009**, *25*, 109–126. [[CrossRef](#)] [[PubMed](#)]
57. Sakaguchi, H.; Ashikaga, T.; Miyazawa, M.; Yoshida, Y.; Ito, Y.; Yoneyama, K.; Hirota, M.; Itagaki, H.; Toyoda, H.; Suzuki, H. Development of an in vitro skin sensitization test using human cell lines; human Cell Line Activation Test (h-CLAT), II. An inter-laboratory study of the h-CLAT. *Toxicol. Vitro.* **2006**, *20*, 774–784. [[CrossRef](#)]
58. Centre, J.R.; Health, I.f.; Protection, C. *EURL ECVAM Recommendation on the Human Cell Line Activation Test (h-CLAT) for Skin Sensitisation Testing*. EUR27022; Publications Office of the European Union: Luxembourg, 2015. [[CrossRef](#)]
59. OECD. *Test No. 442E: In Vitro Skin Sensitisation Assays Addressing the Key Event on Activation of Dendritic Cells on the Adverse Outcome Pathway for Skin Sensitisation*, OECD Guidelines for the Testing of Chemicals, Section 4; OECD Publishing: Paris, France, 2022. [[CrossRef](#)]
60. Chary, A.; Serchi, T.; Moschini, E.; Hennen, J.; Cambier, S.; Ezendam, J.; Blömeke, B.; Gutleb, A.C. An in vitro coculture system for the detection of sensitization following aerosol exposure. *ALTEX-Altern. Anim. Exp.* **2019**, *36*, 403–418. [[CrossRef](#)]
61. Scheurlen, K.M.; Snook, D.L.; Gardner, S.A.; Eichenberger, M.R.; Galandiuk, S. Macrophage differentiation and polarization into an M2-like phenotype using a human monocyte-like THP-1 leukemia cell line. *JoVE (J. Vis. Exp.)* **2021**, e62652. [[CrossRef](#)]
62. Berges, C.; Naujokat, C.; Tinapp, S.; Wieczorek, H.; Höh, A.; Sadeghi, M.; Opelz, G.; Daniel, V. A cell line model for the differentiation of human dendritic cells. *Biochem. Biophys. Res. Commun.* **2005**, *333*, 896–907. [[CrossRef](#)]
63. Larsson, K.; Lindstedt, M.; Borrebaeck, C.A.K. Functional and transcriptional profiling of MUTZ-3, a myeloid cell line acting as a model for dendritic cells. *Immunology* **2006**, *117*, 156–166. [[CrossRef](#)] [[PubMed](#)]
64. Czernek, L.; Chworos, A.; Duechler, M. The Uptake of Extracellular Vesicles is Affected by the Differentiation Status of Myeloid Cells. *Scand. J. Immunol.* **2015**, *82*, 506–514. [[CrossRef](#)] [[PubMed](#)]
65. Galbiati, V.; Marinovich, M.; Corsini, E. Mechanistic understanding of dendritic cell activation in skin sensitization: Additional evidences to support potency classification. *Toxicol. Lett.* **2020**, *322*, 50–57. [[CrossRef](#)]
66. Ogasawara, N.; Kojima, T.; Go, M.; Fuchimoto, J.; Kamekura, R.; Koizumi, J.-i.; Ohkuni, T.; Masaki, T.; Murata, M.; Tanaka, S.; et al. Induction of JAM-A during differentiation of human THP-1 dendritic cells. *Biochem. Biophys. Res. Commun.* **2009**, *389*, 543–549. [[CrossRef](#)] [[PubMed](#)]
67. Yang, Z.; Xiong, H.-R. Culture conditions and types of growth media for mammalian cells. *Biomed. Tissue Cult.* **2012**, *1*, 3–18.
68. Wu, X.; Lin, M.; Li, Y.; Zhao, X.; Yan, F. Effects of DMEM and RPMI 1640 on the biological behavior of dog periosteum-derived cells. *Cytotechnology* **2009**, *59*, 103–111. [[CrossRef](#)]
69. Arora, M. Cell culture media: A review. *Mater. Methods* **2013**, *3*, 24. [[CrossRef](#)]
70. Yao, T.; Asayama, Y. Animal-cell culture media: History, characteristics, and current issues. *Reprod. Med. Biol.* **2017**, *16*, 99–117. [[CrossRef](#)]
71. Chometon, T.Q.; Siqueira, M.d.S.; Sant’anna, J.C.; Almeida, M.R.; Gandini, M.; de Almeida Nogueira, A.C.M.; Antas, P.R.Z. A protocol for rapid monocyte isolation and generation of singular human monocyte-derived dendritic cells. *PLoS ONE* **2020**, *15*, e0231132. [[CrossRef](#)]
72. Lenschow, D.J.; Walunas, T.L.; Bluestone, J.A. CD28/B7 SYSTEM OF T CELL COSTIMULATION. *Annu. Rev. Immunol.* **1996**, *14*, 233–258. [[CrossRef](#)]
73. Chen, J.; Namiki, S.; Toma-Hirano, M.; Miyatake, S.; Ishida, K.; Shibata, Y.; Arai, N.; Arai, K.; Kamogawa-Schifter, Y. The role of CD11b in phagocytosis and dendritic cell development. *Immunol. Lett.* **2008**, *120*, 42–48. [[CrossRef](#)] [[PubMed](#)]
74. Pinet, V.; Vergelli, M.; Martini, R.; Bakke, O.; Long, E.O. Antigen presentation mediated by recycling of surface HLA-DR molecules. *Nature* **1995**, *375*, 603–606. [[CrossRef](#)] [[PubMed](#)]
75. Lechmann, M.; Berchtold, S.; Steinkasserer, A.; Hauber, J. CD83 on dendritic cells: More than just a marker for maturation. *Trends Immunol.* **2002**, *23*, 273–275. [[CrossRef](#)] [[PubMed](#)]
76. Zou, Y.-R.; Kottmann, A.H.; Kuroda, M.; Taniuchi, I.; Littman, D.R. Function of the chemokine receptor CXCR4 in haematopoiesis and in cerebellar development. *Nature* **1998**, *393*, 595–599. [[CrossRef](#)] [[PubMed](#)]

77. Ratajczak, M.Z.; Kucia, M.; Reza, R.; Majka, M.; Janowska-Wieczorek, A.; Ratajczak, J. Stem cell plasticity revisited: CXCR4-positive cells expressing mRNA for early muscle, liver and neural cells 'hide out' in the bone marrow. *Leukemia* **2004**, *18*, 29–40. [[CrossRef](#)]
78. Pituch-Noworolska, A.; Majka, M.; Janowska-Wieczorek, A.; Baj-Krzyworzeka, M.; Urbanowicz, B.; Malec, E.; Ratajczak, M.Z. Circulating CXCR4-positive stem/progenitor cells compete for SDF-1-positive niches in bone marrow, muscle and neural tissues: An alternative hypothesis to stem cell plasticity. *Folia Histochem. Et Cytobiol.* **2003**, *41*, 13–21.
79. Pablos, J.L.; Amara, A.; Bouloc, A.; Santiago, B.; Caruz, A.; Galindo, M.; Delaunay, T.; Virelizier, J.L.; Arenzana-Seisdedos, F. Stromal-Cell Derived Factor Is Expressed by Dendritic Cells and Endothelium in Human Skin. *Am. J. Pathol.* **1999**, *155*, 1577–1586. [[CrossRef](#)]
80. Ceradini, D.J.; Kulkarni, A.R.; Callaghan, M.J.; Tepper, O.M.; Bastidas, N.; Kleinman, M.E.; Capla, J.M.; Galiano, R.D.; Levine, J.P.; Gurtner, G.C. Progenitor cell trafficking is regulated by hypoxic gradients through HIF-1 induction of SDF-1. *Nat. Med.* **2004**, *10*, 858–864. [[CrossRef](#)]
81. Minami, H.; Nagaharu, K.; Nakamori, Y.; Ohishi, K.; Shimojo, N.; Kageyama, Y.; Matsumoto, T.; Sugimoto, Y.; Tawara, I.; Masuya, M.; et al. CXCL12–CXCR4 Axis Is Required for Contact-Mediated Human B Lymphoid and Plasmacytoid Dendritic Cell Differentiation but Not T Lymphoid Generation. *J. Immunol.* **2017**, *199*, 2343–2355. [[CrossRef](#)]
82. Umemoto, E.; Otani, K.; Ikeno, T.; Garcia, N.V.; Hayasaka, H.; Bai, Z.; Jang, M.H.; Tanaka, T.; Nagasawa, T.; Ueda, K.; et al. Constitutive Plasmacytoid Dendritic Cell Migration to the Splenic White Pulp Is Cooperatively Regulated by CCR7- and CXCR4-Mediated Signaling. *J. Immunol.* **2012**, *189*, 191–199. [[CrossRef](#)]
83. Delgado, E.; Finkel, V.; Baggiolini, M.; Mackay, C.R.; Steinman, R.M.; Granelli-Piperno, A. Mature Dendritic Cells Respond to SDF-1, but not to Several  $\beta$ -Chemokines. *Immunobiology* **1998**, *198*, 490–500. [[CrossRef](#)] [[PubMed](#)]
84. Ricart, B.G.; John, B.; Lee, D.; Hunter, C.A.; Hammer, D.A. Dendritic Cells Distinguish Individual Chemokine Signals through CCR7 and CXCR4. *J. Immunol.* **2011**, *186*, 53–61. [[CrossRef](#)] [[PubMed](#)]
85. Bleul, C.C.; Wu, L.; Hoxie, J.A.; Springer, T.A.; Mackay, C.R. The HIV coreceptors CXCR4 and CCR5 are differentially expressed and regulated on human T lymphocytes. *Proc. Natl. Acad. Sci. USA* **1997**, *94*, 1925–1930. [[CrossRef](#)]
86. Nukada, Y.; Ashikaga, T.; Sakaguchi, H.; Sono, S.; Mugita, N.; Hirota, M.; Miyazawa, M.; Ito, Y.; Sasa, H.; Nishiyama, N. Predictive performance for human skin sensitizing potential of the human cell line activation test (h-CLAT). *Contact Dermat.* **2011**, *65*, 343–353. [[CrossRef](#)] [[PubMed](#)]
87. Takenouchi, O.; Miyazawa, M.; Saito, K.; Ashikaga, T.; Sakaguchi, H. Predictive performance of the human Cell Line Activation Test (h-CLAT) for lipophilic chemicals with high octanol-water partition coefficients. *J. Toxicol. Sci.* **2013**, *38*, 599–609. [[CrossRef](#)] [[PubMed](#)]
88. Alloati, A.; Kotsias, F.; Magalhaes, J.G.; Amigorena, S. Dendritic cell maturation and cross-presentation: Timing matters! *Immunol. Rev.* **2016**, *272*, 97–108. [[CrossRef](#)]
89. Takahashi, M.; Kobayashi, Y. Cytokine production in association with phagocytosis of apoptotic cells by immature dendritic cells. *Cell. Immunol.* **2003**, *226*, 105–115. [[CrossRef](#)]
90. Xia, H.; Wang, Y.; Dai, J.; Zhang, X.; Zhou, J.; Zeng, Z.; Jia, Y. Selenoprotein K Is Essential for the Migration and Phagocytosis of Immature Dendritic Cells. *Antioxidants* **2022**, *11*, 1264. [[CrossRef](#)]
91. Kiama, S.; Cochand, L.; Karlsson, L.; Nicod, L.; Gehr, P. Evaluation of phagocytic activity in human monocyte-derived dendritic cells. *J. Aerosol Med.* **2001**, *14*, 289–299. [[CrossRef](#)] [[PubMed](#)]
92. Tait Wojno, E.D.; Hunter, C.A.; Stumhofer, J.S. The Immunobiology of the Interleukin-12 Family: Room for Discovery. *Immunity* **2019**, *50*, 851–870. [[CrossRef](#)]
93. Riemann, H.; Schwarz, A.; Grabbe, S.; Aragane, Y.; Luger, T.A.; Wsocka, M.; Kubin, M.; Trinchieri, G.; Schwarz, T. Neutralization of IL-12 in vivo prevents induction of contact hypersensitivity and induces hapten-specific tolerance. *J. Immunol.* **1996**, *156*, 1799–1803. [[CrossRef](#)]
94. Ade, N.; Antonios, D.; Kerdine-Romer, S.; Boislevé, F.; Rousset, F.; Pallardy, M. NF- $\kappa$ B Plays a Major Role in the Maturation of Human Dendritic Cells Induced by NiSO<sub>4</sub> but not by DNCB. *Toxicol. Sci.* **2007**, *99*, 488–501. [[CrossRef](#)]
95. Antonios, D.; Rousseau, P.; Larangé, A.; Kerdine-Römer, S.; Pallardy, M. Mechanisms of IL-12 Synthesis by Human Dendritic Cells Treated with the Chemical Sensitizer NiSO<sub>4</sub>. *J. Immunol.* **2010**, *185*, 89–98. [[CrossRef](#)] [[PubMed](#)]
96. Aiba, S.; Manome, H.; Nakagawa, S.; Mollah, Z.U.A.; Mizuashi, M.; Ohtani, T.; Yoshino, Y.; Tagami, H. p38 Mitogen-activated Protein Kinase and Extracellular Signal-regulated Kinases Play Distinct Roles in the Activation of Dendritic Cells by Two Representative Haptens, NiCl<sub>2</sub> and 2,4-dinitrochlorobenzene. *J. Invest. Dermatol.* **2003**, *120*, 390–399. [[CrossRef](#)]
97. Hayashi, M.; Higashi, K.; Kato, H.; Kaneko, H. Assessment of Preferential Th1 or Th2 Induction by Low-Molecular-Weight Compounds Using a Reverse Transcription–Polymerase Chain Reaction Method: Comparison of Two Mouse Strains, C57BL/6 and Balb/c. *Toxicol. Appl. Pharmacol.* **2001**, *177*, 38–45. [[CrossRef](#)] [[PubMed](#)]
98. Warbrick, E.V.; Dearman, R.J.; Basketter, D.A.; Kimber, I. Analysis of interleukin 12 protein production and mRNA expression in mice exposed topically to chemical allergens. *Toxicology* **1999**, *132*, 57–66. [[CrossRef](#)]
99. Xu, B.; Aoyama, K.; Kitani, A.; Matsuyama, T.; Matsushita, T. RT-PCR analysis of in vivo cytokine profiles in murine allergic contact dermatitis to DNCB. *Toxicol. Methods* **1996**, *6*, 23–31. [[CrossRef](#)]
100. Sándor, N.; Kristóf, K.; Paréj, K.; Pap, D.; Erdei, A.; Bajtay, Z. CR3 is the dominant phagocytotic complement receptor on human dendritic cells. *Immunobiology* **2013**, *218*, 652–663. [[CrossRef](#)] [[PubMed](#)]

101. Li, Z.; Ju, X.; Silveira, P.A.; Abadir, E.; Hsu, W.-H.; Hart, D.N.; Clark, G.J. CD83: Activation marker for antigen presenting cells and its therapeutic potential. *Front. Immunol.* **2019**, *10*, 1312. [[CrossRef](#)] [[PubMed](#)]
102. Zraggen, S.; Huggenberger, R.; Kerl, K.; Detmar, M. An important role of the SDF-1/CXCR4 axis in chronic skin inflammation. *PLoS ONE* **2014**, *9*, e93665. [[CrossRef](#)]
103. Gallego, C.; Vétillard, M.; Calmette, J.; Roriz, M.; Marin-Esteban, V.; Evrard, M.; Aknin, M.-L.; Pionnier, N.; Lefrançois, M.; Mercier-Nomé, F. CXCR4 signaling controls dendritic cell location and activation at steady state and in inflammation. *Blood* **2021**, *137*, 2770–2784. [[CrossRef](#)] [[PubMed](#)]
104. Enk, A.H.; Jonuleit, H.; Saloga, J.; Knop, J. Dendritic cells as mediators of tumor-induced tolerance in metastatic melanoma. *Int. J. Cancer* **1997**, *73*, 309–316. [[CrossRef](#)]
105. Kim, C.W.; Kim, K.-D.; Lee, H.K. The role of dendritic cells in tumor microenvironments and their uses as therapeutic targets. *BMB Rep.* **2021**, *54*, 31. [[CrossRef](#)] [[PubMed](#)]

**Disclaimer/Publisher’s Note:** The statements, opinions and data contained in all publications are solely those of the individual author(s) and contributor(s) and not of MDPI and/or the editor(s). MDPI and/or the editor(s) disclaim responsibility for any injury to people or property resulting from any ideas, methods, instructions or products referred to in the content.